

~~RESTRICTED~~

N62 60276

RM E9K25a

NACA RM E9K25a



CASE FILE  
COPY

# RESEARCH MEMORANDUM

TRANSIENT OPERATING CHARACTERISTICS OF A TURBOJET ENGINE  
WHEN SUBJECTED TO STEP CHANGES IN FUEL FLOW

By Arthur H. Bell and J. Elmo Farmer

Lewis Flight Propulsion Laboratory  
Cleveland, Ohio

CLASSIFICATION CANCELLED	
Authority <u>Crowley</u>	Date <u>12-14-53</u>
By <u>T. C. F.</u>	Release form no. <u>1935</u>

NATIONAL ADVISORY COMMITTEE  
FOR AERONAUTICS

WASHINGTON

February 20, 1950

~~RESTRICTED~~

NATIONAL ADVISORY COMMITTEE FOR AERONAUTICS

RESEARCH MEMORANDUM

TRANSIENT OPERATING CHARACTERISTICS OF A TURBOJET  
ENGINE WHEN SUBJECTED TO STEP CHANGES IN  
FUEL FLOW

By Arthur H. Bell and J. Elmo Farmer

SUMMARY

An investigation was conducted on a typical centrifugal-compressor-type turbojet engine to determine the operating characteristics during changes in engine speed resulting from sudden changes in fuel flow. The experimental data presented are suitable for use in the study of control problems associated with transient operation. The data show the variations with time of engine speed, thrust, fuel flow, and critical gas and material temperatures caused by sudden changes in fuel flow.

The investigation shows that the gas temperature at the tail-cone exit indicates the approximate turbine-blade temperature during periods of acceleration and deceleration. The time required for rotor speed to become stable was approximately the same for both accelerations and decelerations of the same magnitude over the same range of speeds.

INTRODUCTION

The design of automatic controls for a gas-turbine engine requires knowledge of a number of characteristic relations for the engine under consideration. The rate of change of engine speed with various changes in fuel flow, for instance, must be known in order that the proper choice of constants may be made for a speed control to prevent hunting or overshooting. Temperature-acceleration relations must be known so that controls can be designed to protect the engine against excessive temperatures during acceleration. Other characteristics, such as blow-out limits, must be known so controls can be designed to insure continuous operation of the engine during acceleration and deceleration.

Experimental data obtained at the NACA Lewis laboratory describe the engine operating characteristics during transient conditions of a centrifugal-compressor-type turbojet engine typical of current design practice. The investigation included observation of engine operation at sea-level conditions during periods of acceleration and deceleration over wide ranges of engine speed.

The acceleration and deceleration data were obtained in such a manner that they are characteristic of the engine alone and essentially independent of the external fuel system and engine operator. The engine fuel system was modified to provide for a change of fuel flow in a well-defined single step by installing a second throttle and solenoid valve in a bypass line around the main engine throttle. This alteration in the fuel system made possible very rapid changes in the one independent variable, fuel flow. During periods of acceleration and deceleration, measurements were made of the variation with time of engine speed, thrust, various gas temperatures, and turbine-blade temperature. The data presented herein are suitable for use in the study of control problems associated with transient operation of turbojet engines having centrifugal compressors.

## APPARATUS AND PROCEDURE

### Engine

The turbojet engine used has a centrifugal compressor with 14 can-type burners, a single-stage turbine, and a fixed-area exhaust nozzle. The maximum rated engine speed is 11,500 rpm. In this investigation, the engine is considered typical of current design practice and performance for production centrifugal-compressor-type turbojet engines. The test stand was of the static-thrust type with a pendulum mounting.

### Fuel System

The engine fuel system was altered to make possible very rapid changes in fuel flow. This alteration allowed the acceleration and deceleration characteristics of the engine to be determined independently of external fuel-system characteristics and operating technique.

The fuel system used included an auxiliary throttle and a solenoid valve installed in series in a bypass line around the main throttle. With the solenoid valve closed, the main throttle was adjusted to give a desired lower engine speed. The solenoid valve was then opened and the auxiliary throttle adjusted to pass additional fuel to give a selected higher engine speed. The fuel flows for any two steady-state engine speeds could thus be established and the necessary rapid change in fuel flow for acceleration or deceleration between the two engine speeds was obtained by opening or closing the solenoid valve. The rapid changes in fuel flow obtained in this manner will be referred to hereinafter as "step changes" although the changes were not instantaneous.

Fuel flow was measured by use of an orifice in the main fuel line and a gage, which measured the pressure drop across the orifice. A preliminary investigation of the response rate of the fuel-flow-measuring instrumentation showed that the instrumentation was capable of following much more rapid flow-rate changes than those encountered during the engine runs. The time required for fuel flow to change from one value to another, however, was found to vary with the length of hose downstream of the orifice and with the amount of outlet restriction. It is therefore presumed that the indicated time required for the fuel flow to change from one value to another when the solenoid valve in the bypass line was operated was primarily caused by the fuel-system configuration rather than by any limitation in the measuring equipment.

#### Turbine-Blade Thermocouple Installation

Turbine-blade temperatures were indicated by one thermocouple in the leading edge of each of six turbine blades. A hole was drilled in each of the blades from the bottom of the root to the leading edge. Chromel and alumel wires were passed through a two-hole Alundum insulation tube, which was then encased in a stainless-steel tube. This assembly was passed through the drilled hole in a turbine blade, as shown in figure 1. The thermocouple junction was then welded into the leading edge of the blade and the surface finished to the original contour of the blade. The thermocouple junctions were located midway between the blade root and the blade tip.

The tubes containing the thermocouple wires were attached to the fir-tree root (fig. 1), and then were passed along the downstream face of the turbine wheel to a terminal block at the hub. The tubes were fastened to the wheel with small straps spot-welded to the wheel. The installation on the turbine wheel is shown in figure 2.

Six pairs of chromel-alumel leads were installed from the terminal block through holes in the centers of the turbine and compressor shafts to a slip-ring mechanism at the forward end of the engine. The slip-ring mechanism (fig. 3) consisted of 12 copper rings on a shaft connected directly to the engine compressor shaft. Brushes made of copper were mounted on a bakelite block, which was pivoted in such a manner that the brushes could be lifted from the slip rings when not in use. This arrangement was provided to decrease wear on the slip rings and brushes. The brush pressure during contact was adjusted to approximately 40 pounds per square inch. A steam-heated uniform-temperature box was provided at the end of the slip-ring assembly to house the junctions between the chromel-alumel lead wires and the copper wires that led to the slip rings. The circuit was completed, as shown in figure 4, through a selector switch and the uniform-temperature box to a recording potentiometer.

Because only one potentiometer was used for blade-temperature measurement, it was possible to use only one of the blade thermocouples for any given acceleration or deceleration run. The indicated temperatures of all six thermocouples were so similar that if trouble was experienced with one thermocouple another could be used without stopping the engine to make repairs.

#### Gas-Temperature Thermocouple Installation

All gas temperatures were measured with bare chromel-alumel thermocouples of 18-gage wire. Figure 5 is an outline of the engine showing axial positions of temperature-measuring stations on the engine. The burner-exit gas temperature was obtained from one of the burners upstream of the nozzle diaphragm. The gas temperature at the tail-cone exit was an average reading obtained by connecting 14 thermocouples in parallel to a single indicator. These 14 thermocouples extended radially 2 inches into the tail pipe and were equally spaced circumferentially about the tail pipe. The gas temperature at the tail-pipe exit was obtained from one thermocouple at the center of the gas stream.

#### Thrust Meter

Engine thrust was measured by strain gages mounted on a thrust link. The strain-gage circuit was connected to a self-balancing potentiometer, the drive motor of which was connected to an indicating

dial. A check run on the response rate of this system showed it to be capable of following thrust changes during acceleration and deceleration with negligible lag.

### Data Recording Apparatus

Data for the acceleration and deceleration runs were obtained by photographing a panel of instruments with a motion-picture camera at the rate of 12 frames per second. In analyzing the data, readings from many of the frames representing nearly linear rates of change were omitted to save time. A photograph of the instrument panel, taken while the engine was inoperative, is shown in figure 6. The temperature indicators used with the gas-temperature thermocouples were of the millivoltmeter type with fixed-resistance leads. A tachometer indicated engine speed in revolutions per minute, and time was indicated by a clock reading in thousandths of a minute. The horizontal scale of the self-balancing recording potentiometer was placed at the bottom of the panel so that the indication of turbine-blade temperature could be photographed in addition to the recording on the chart. Other instruments shown were not used during the investigation reported.

## RESULTS AND DISCUSSION

### Acceleration

Results of the acceleration runs are presented in figure 7 and the change in engine speed that corresponds to the data of each part is given in table I. Each part of figure 7 consists of seven curves, four representing burner-exit, turbine-blade, tail-cone-exit, and tail-pipe-exit temperatures and three representing engine speed, fuel flow, and thrust as functions of time. The zero point on the time scale corresponds with the instant of opening or closing of the solenoid valve in the fuel-system bypass line. The four temperature curves were not corrected to standard conditions inasmuch as the proper corrections for turbine-blade temperatures were not known. The engine-speed, fuel-flow, and thrust curves represent data that have been corrected to NACA standard sea-level conditions by the use of  $\delta$  (ratio of engine-inlet static pressure to NACA standard sea-level pressure) and  $\theta$  (ratio of observed compressor-inlet temperature to NACA standard sea-level temperature). The various values of  $\delta$  and  $\theta$  are included in the figure sublegends.

An arrow was placed on each curve at the point at which the slope became approximately zero to make it easier to visualize the time necessary for the different variables to reach steady-state conditions. The curve of fuel flow against time in figures 7(e), 7(j), 7(o), and 7(p) shows a tendency to level off before reaching a maximum value and then to increase more slowly toward the steady-state value. This peculiarity was observed only where the changes in fuel flow were exceptionally large and is attributed to the fact that the output of the engine-driven fuel pump increased as the engine speed accelerated.

Inasmuch as the temperature curves were obtained by the use of bare-wire thermocouples and the necessarily small amount of instrumentation, it is emphasized that the indicated temperatures may be somewhat different from the true station temperatures. The shapes of the curves are significant, however, and a number of interesting trends can be observed. For example, the curves show that the gas temperature at the tail-pipe exit in almost all cases overshoots soon after an increase in fuel flow is made and then gradually drops back to an equilibrium level as engine speed increases to a steady value. The curves of gas temperature at the tail-cone exit show, however, that, in general, overshooting took place only when the step change in fuel flow was large and the initial engine speed was 8000 rpm or less. The gas temperature at the burner exit did not overshoot appreciably with any step change in fuel flow, except when engine speed was below one-half rated speed and fuel flow was suddenly increased to the rated-speed value, as shown in figure 7(o). The turbine-blade temperatures only momentarily exceed final steady-state values when the burner-exit gas temperatures overshoot.

Analysis of these temperature trends leads to the following hypothesis: Immediately after fuel flow is suddenly increased, a large portion of the fuel increment passes through the burners and burns in the tail pipe. As engine speed (and therefore air flow) increases, the zone of secondary burning moves farther upstream, until as the speed approaches an equilibrium value all burning takes place in the burner. It is apparent that during the process of engine acceleration, gas temperatures measured in the tail pipe are not indicative of turbine-blade temperatures. The tail-pipe gas temperature may rise considerably above its final steady-state value without any accompanying overshooting of turbine-blade temperature. At an engine speed of 8000 rpm (uncorrected), suddenly increasing fuel flow to the maximum-rated-speed value did not cause turbine-blade temperatures to exceed the final steady-state value (fig. 7(e)). At 7000 rpm (uncorrected), suddenly increasing fuel flow to its maximum-rated-speed value caused turbine-blade temperatures to overshoot by about 50° F

(fig. 7(p)). The curves of turbine-blade temperature (fig. 7) show about the same trends as the gas temperature at the tail-cone exit.

As mentioned previously, the turbine-blade temperature was measured at a point very near the leading-edge surface. Because the trailing edge of the blade is thinner than the leading edge, it appears logical that the trailing edge would respond more quickly to changes in gas temperature than the leading edge. An examination of the temperature curves indicates, however, that the leading-edge temperature responds almost as quickly as the bare-wire thermocouples used to measure gas temperatures. It therefore appears likely that the rate of temperature change of the trailing edge cannot be much greater than that of the leading edge. The trailing-edge temperature would therefore not be expected to overshoot appreciably more than the leading-edge temperature.

#### Deceleration

The results of the deceleration runs are presented in figure 8 and the change in engine speed that corresponds to the data of each part is given in table II. These figures are plotted in the same manner as the acceleration curves. Although engine speed drops off rapidly as soon as fuel flow is reduced, the time required for speed to reach equilibrium is of the same order of magnitude as the time required for acceleration through the same speed range. The measured temperatures decreased smoothly during deceleration. It might be expected that the temperatures during deceleration would reach intermediate values lower than the final value, and then increase to an equilibrium value inasmuch as fuel-air ratio is momentarily reduced below the final steady-state value when the fuel flow is suddenly decreased. However, no such undershooting was observed; instead, the temperatures in all cases decreased gradually to the new equilibrium values. It is presumed that this apparent absence of undershooting may be caused by radiation to the thermocouples from the flame in the burners and from nearby metal surfaces having appreciable thermal lag.

#### General Performance

The engine performed in a stable and uniform manner throughout the entire investigation except when attempts were made to accelerate from engine speeds below 5000 rpm to rated engine speed by changing fuel-flow rate from the low to the high value in one step. Under such conditions, turbine speed either failed to increase or decreased

for an appreciable length of time (3 to 5 sec) before beginning to increase toward the rated-speed value. This phenomenon may be attributed to very poor combustion efficiency resulting from the momentary over-rich fuel-air mixture. No instances of complete engine blow-out occurred during deceleration even when the fuel flow was rapidly reduced from the maximum value to that required for idling.

#### SUMMARY OF RESULTS

An investigation conducted on a typical centrifugal-compressor-type turbojet engine to determine the effect of step changes in fuel flow on engine operating conditions gave the following results:

1. Gas-temperature measurement at the tail-cone exit indicated approximate turbine-blade temperature during periods of acceleration and deceleration.
2. Time required for rotor speed to reach equilibrium was approximately the same for accelerations and decelerations of the same magnitude over the same range of speeds.

Lewis Flight Propulsion Laboratory,  
National Advisory Committee for Aeronautics,  
Cleveland, Ohio.

TABLE I - ENGINE SPEEDS AT BEGINNING AND END  
OF EACH ACCELERATION

Figure	Uncorrected engine speed, rpm	
	Beginning of acceleration	End of acceleration
7(a)	8,000	8,500
7(b)	8,000	9,000
7(c)	8,000	9,500
7(d)	8,000	11,000
7(e)	8,000	11,500
7(f)	9,000	9,500
7(g)	9,000	10,000
7(h)	9,000	10,500
7(i)	9,000	11,000
7(j)	9,000	11,500
7(k)	10,000	10,500
7(l)	10,000	11,000
7(m)	10,000	11,500
7(n)	11,000	11,500
7(o)	5,000	11,500
7(p)	7,000	11,500



TABLE II - ENGINE SPEEDS AT BEGINNING AND END  
OF EACH DECELERATION

Figure	Uncorrected engine speed, rpm	
	Beginning of deceleration	End of deceleration
8(a)	11,500	11,000
8(b)	11,500	10,500
8(c)	11,500	10,000
8(d)	11,500	5,000
8(e)	11,000	10,500
8(f)	11,000	10,000
8(g)	10,500	10,000
8(h)	10,500	9,000
8(i)	10,000	9,500
8(j)	10,000	9,000
8(k)	9,500	9,000
8(l)	9,000	8,500
8(m)	9,000	8,000



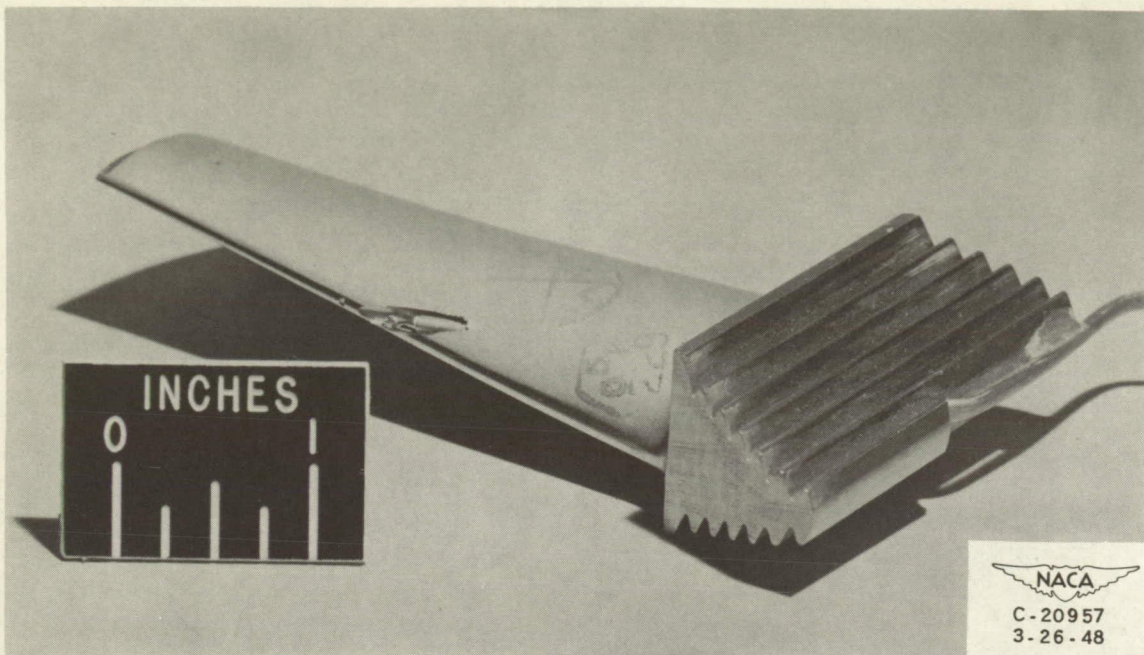


Figure 1. - Turbine-blade thermocouple installation before welding and fairing of leading edge.

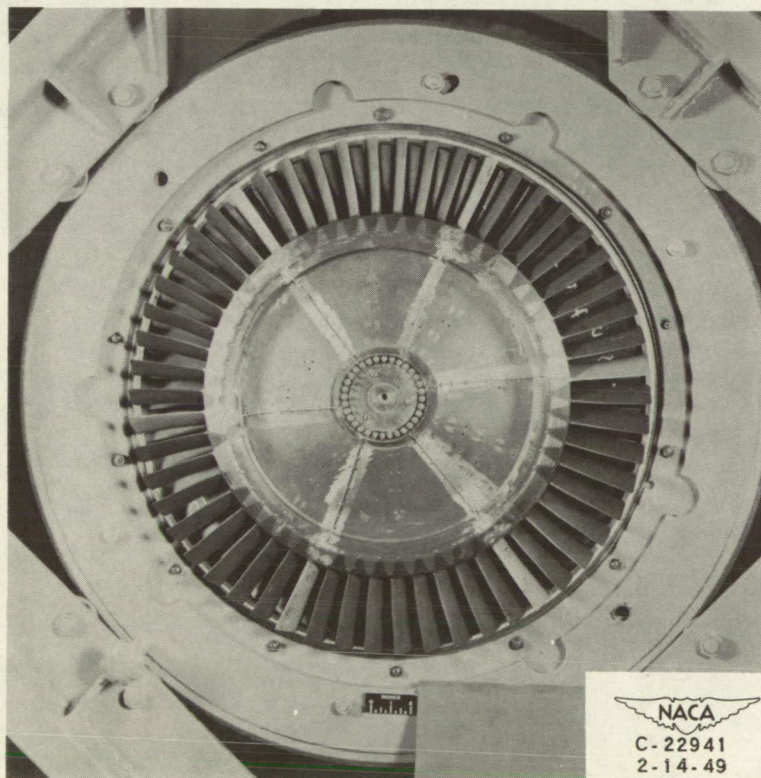


Figure 2. - Turbine wheel showing thermocouple leads and terminal block.

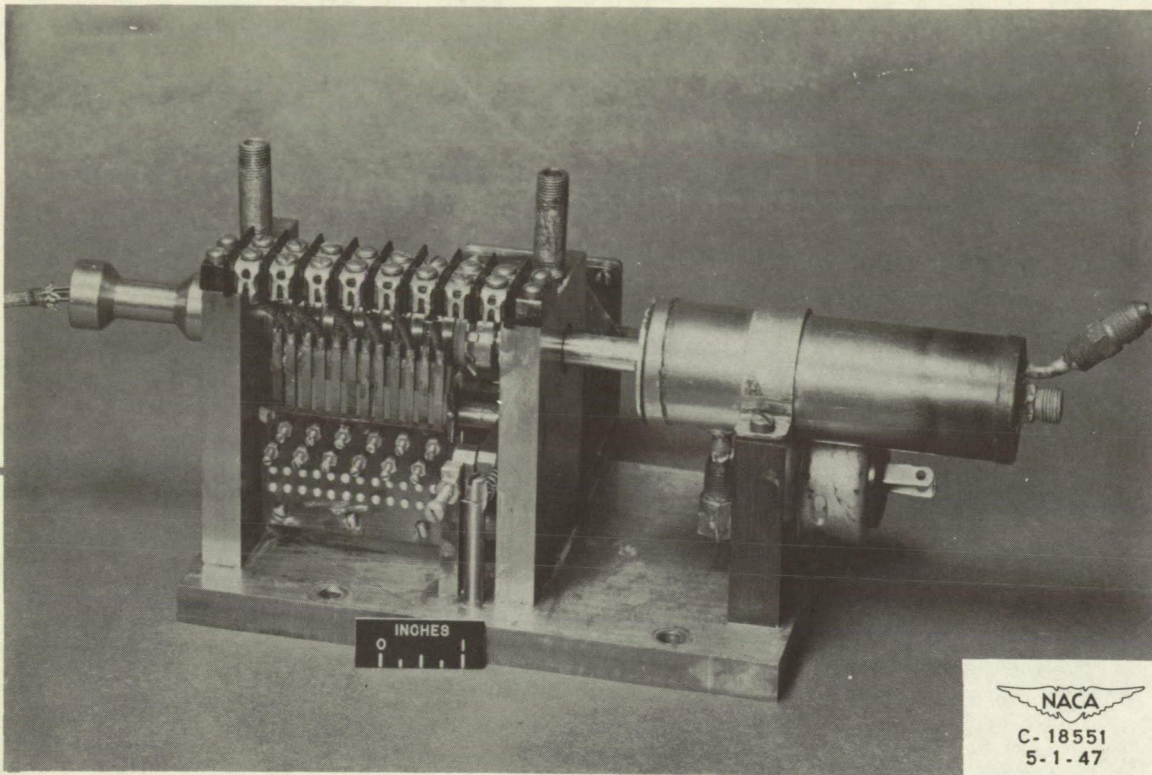


Figure 3. - Slip-ring mechanism and uniform-temperature box for connecting turbine-blade thermocouples to potentiometer.

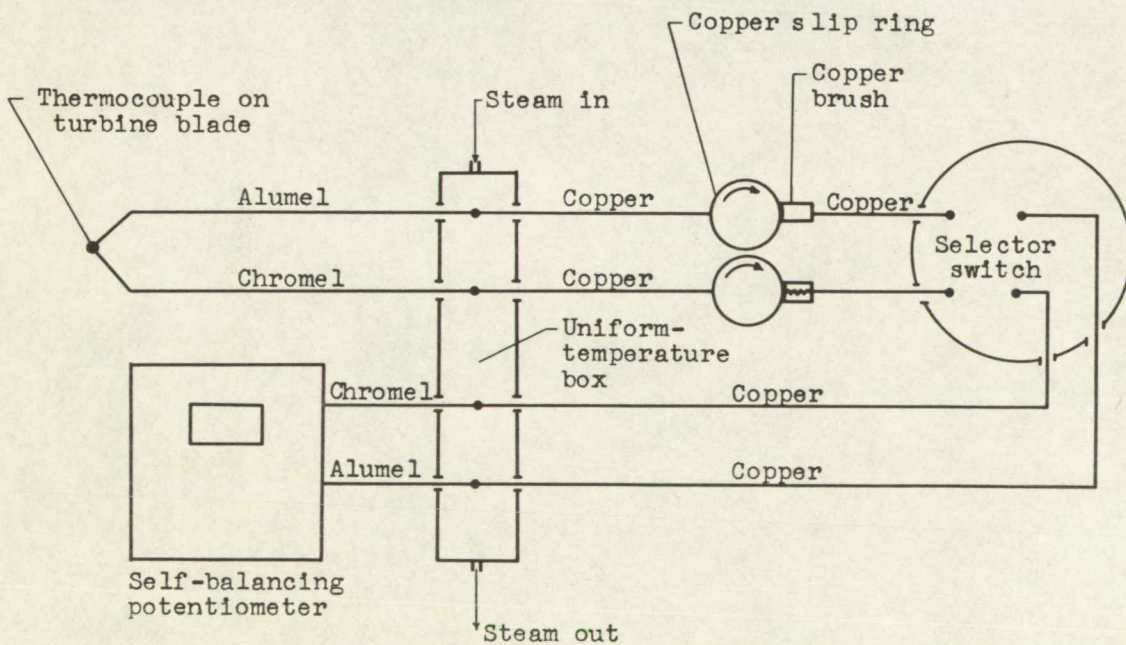


Figure 4. - Schematic diagram of thermocouple installation for measuring turbine-blade temperatures.

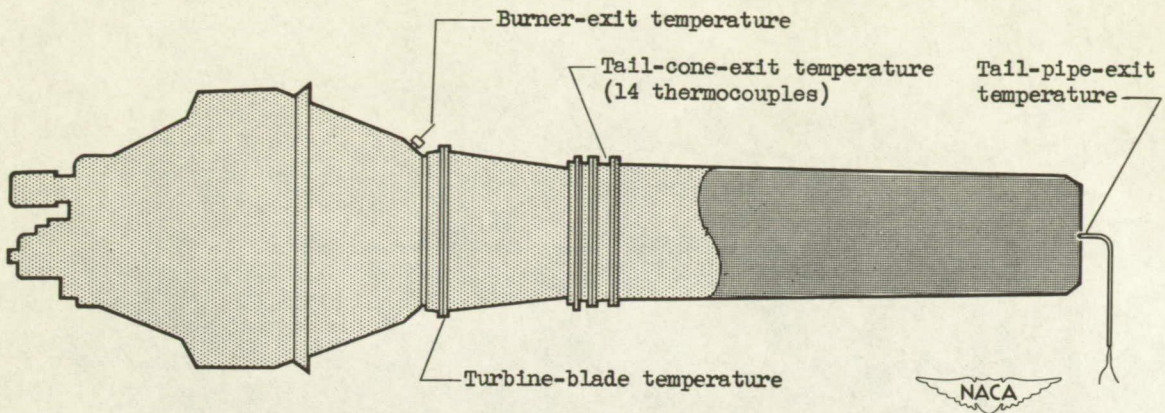


Figure 5. - Axial positions of temperature-measuring stations on engine.

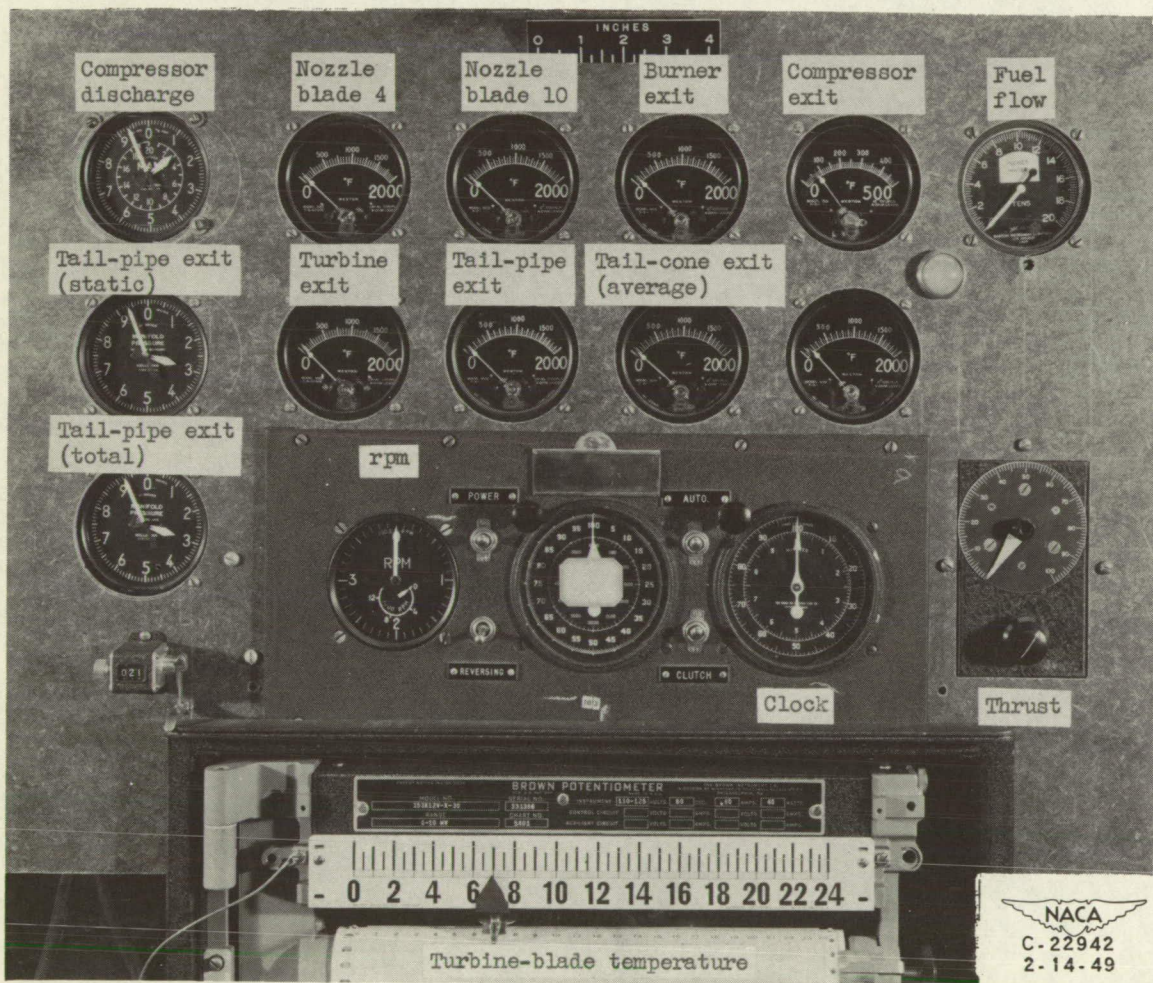
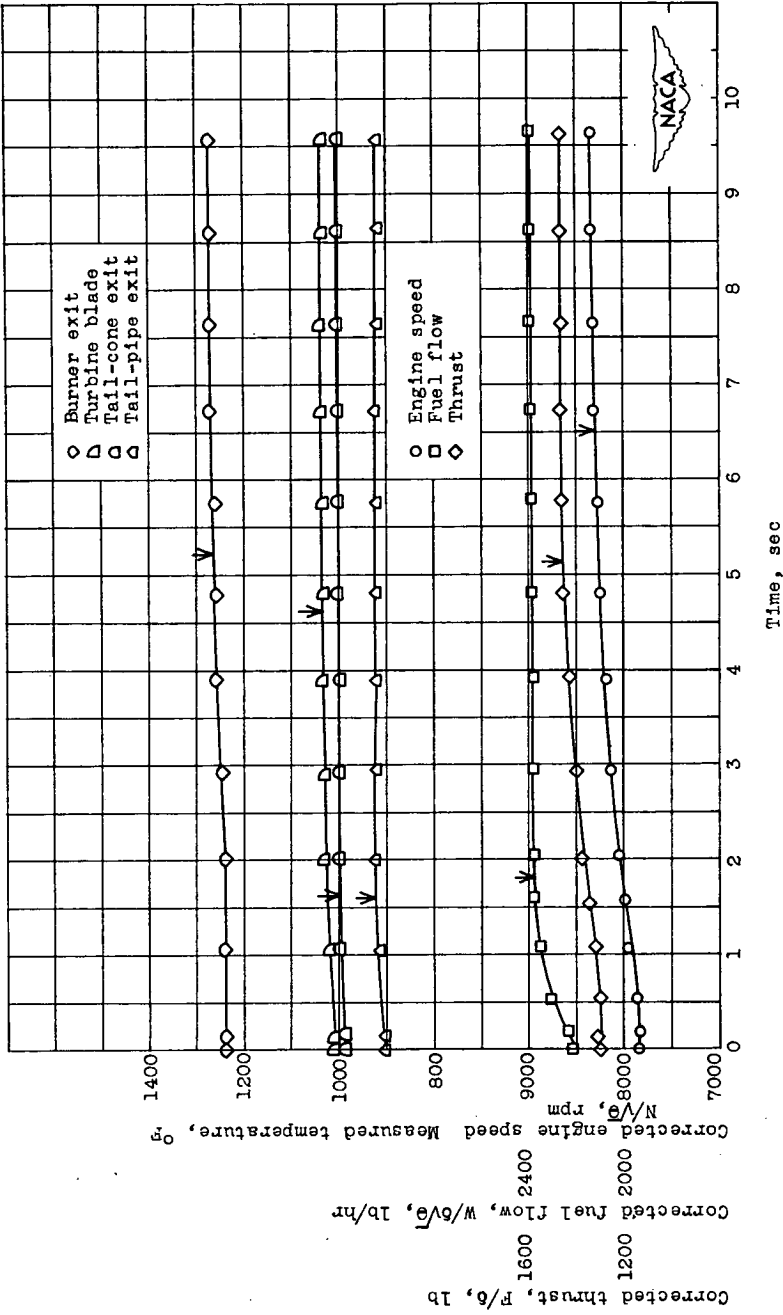
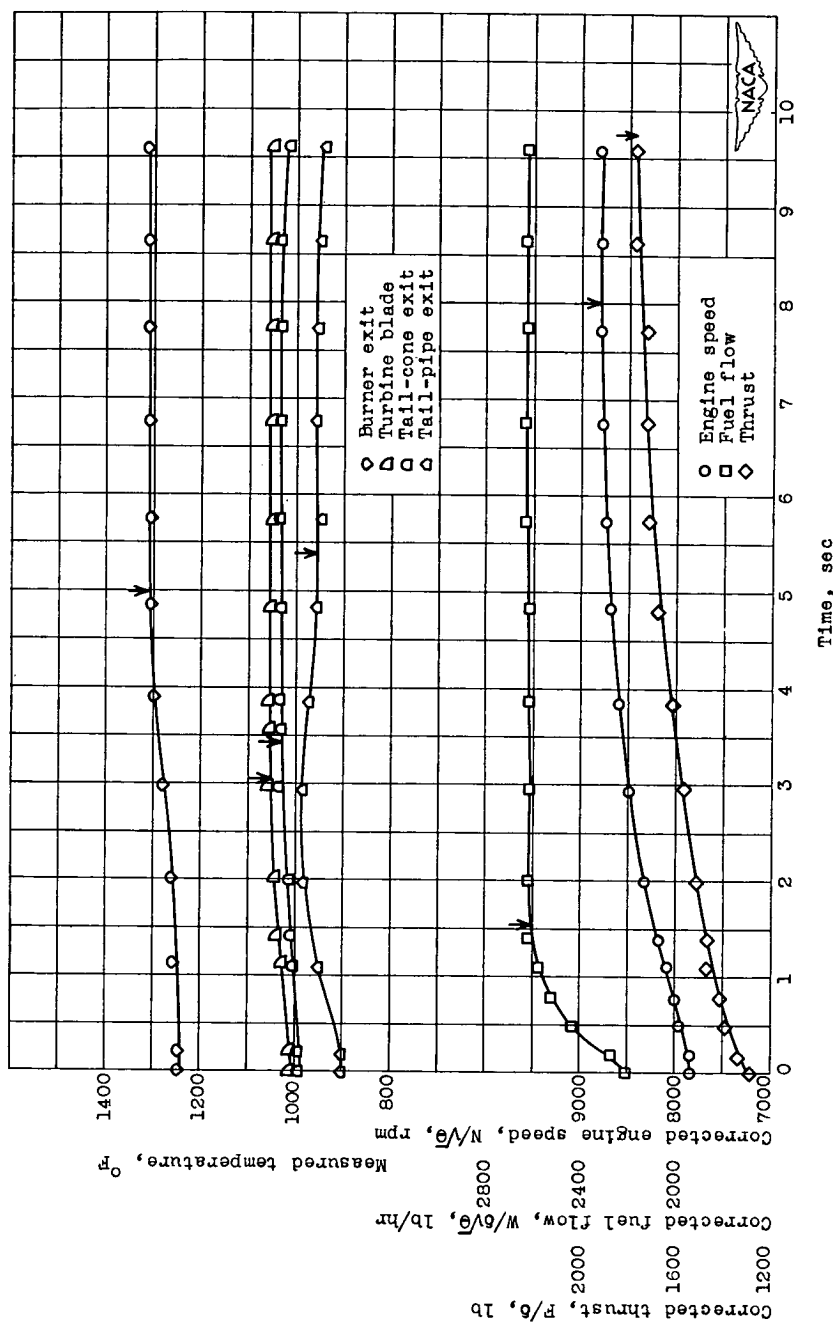


Figure 6. - Instrument panel used for photographically obtaining data.

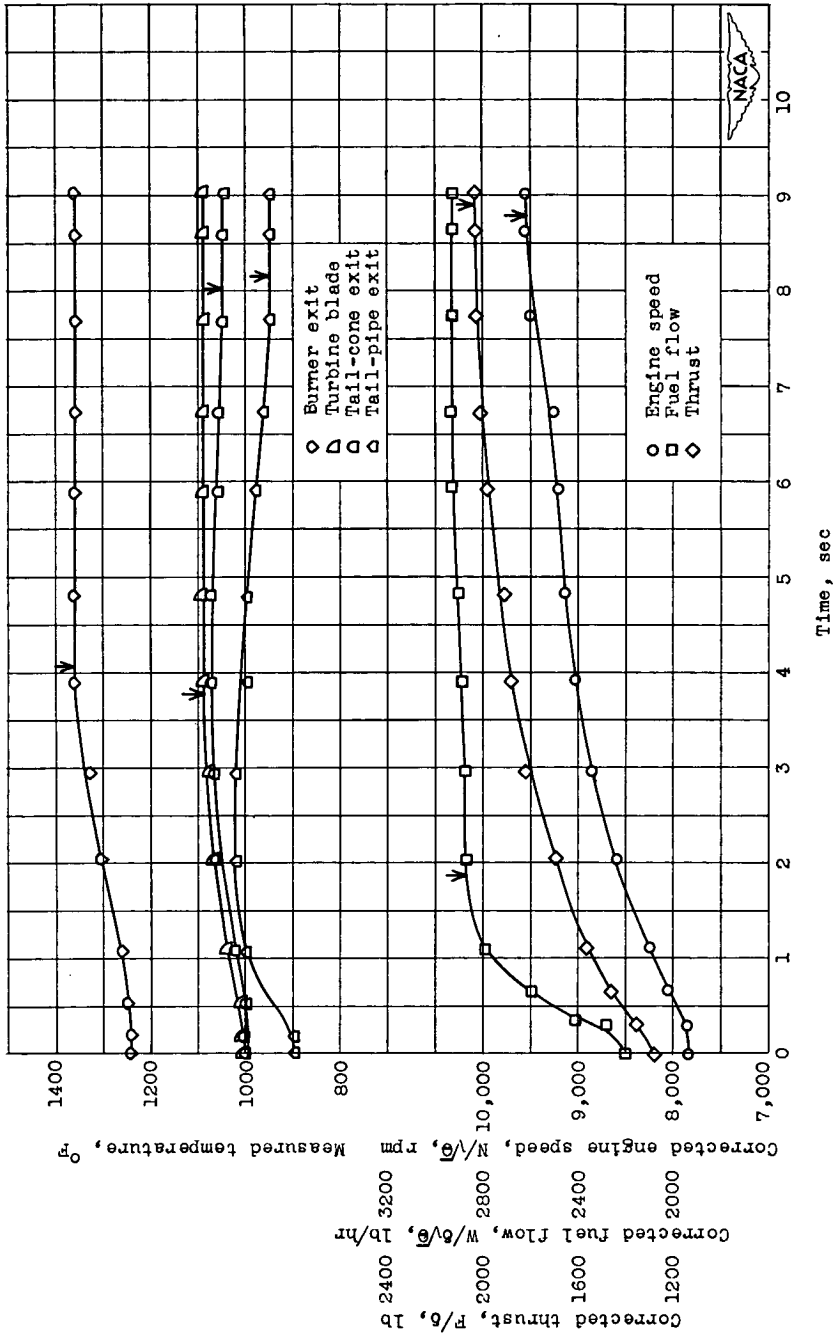


(a) Acceleration, 8000 to 8500 rpm;  $\sqrt{6}$ , 1.020;  $\delta$ , 0.974.  
 Figure 7. - Acceleration characteristics with step change in fuel flow corresponding to change in uncorrected engine speed. Arrows indicate time at which equilibrium is reached.



(b) Acceleration, 8000 to 9000 rpm;  $\sqrt{\theta}$ , 1.020;  $\delta$ , 0.974.

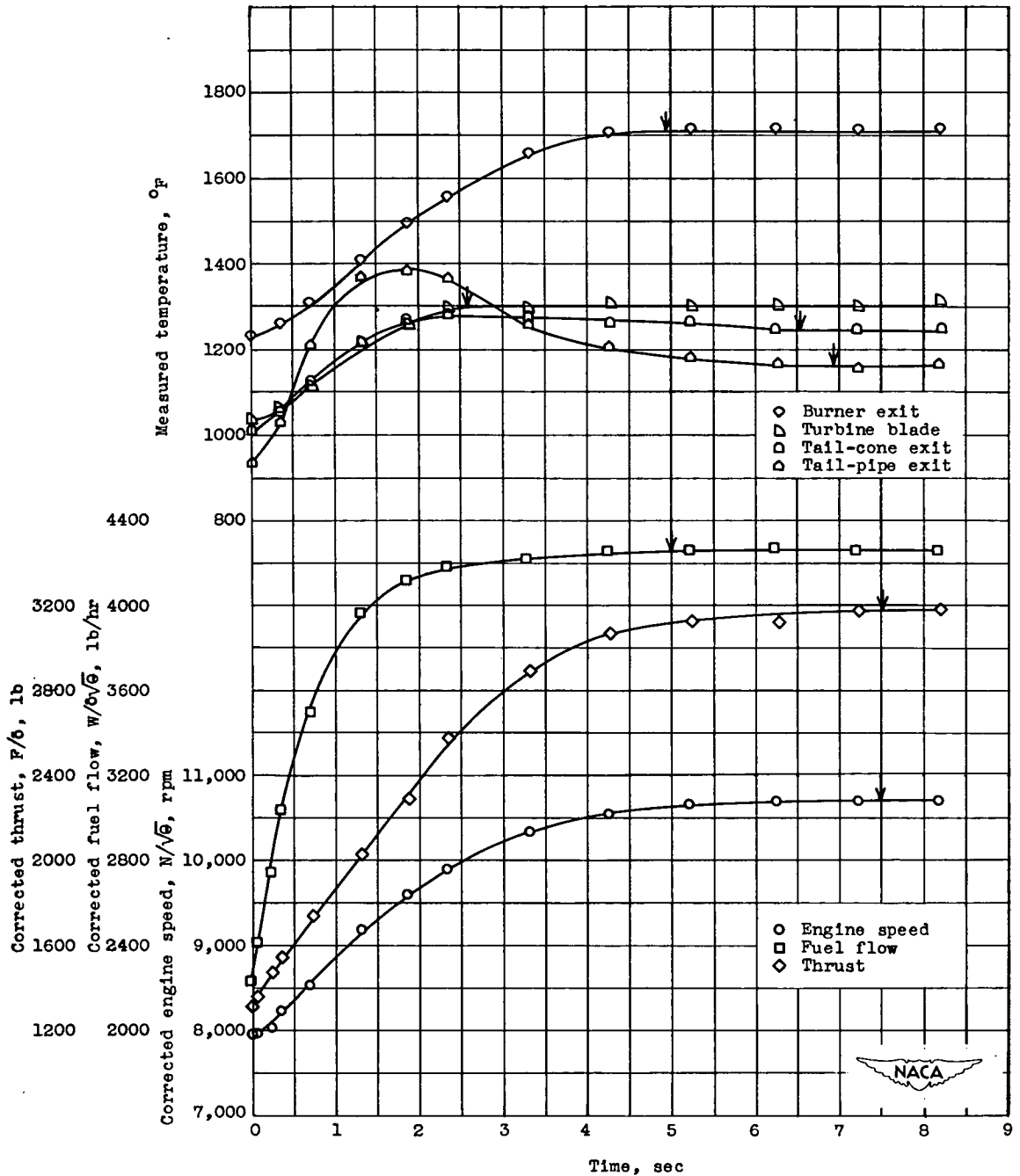
Figure 7. - Continued. Acceleration characteristics with step change in fuel flow corresponding to change in uncorrected engine speed. Arrows indicate time at which equilibrium is reached.



(c) Acceleration, 8000 to 9500 rpm;  $\sqrt{\theta}$ , 1.020;  $\theta$ , 0.974.

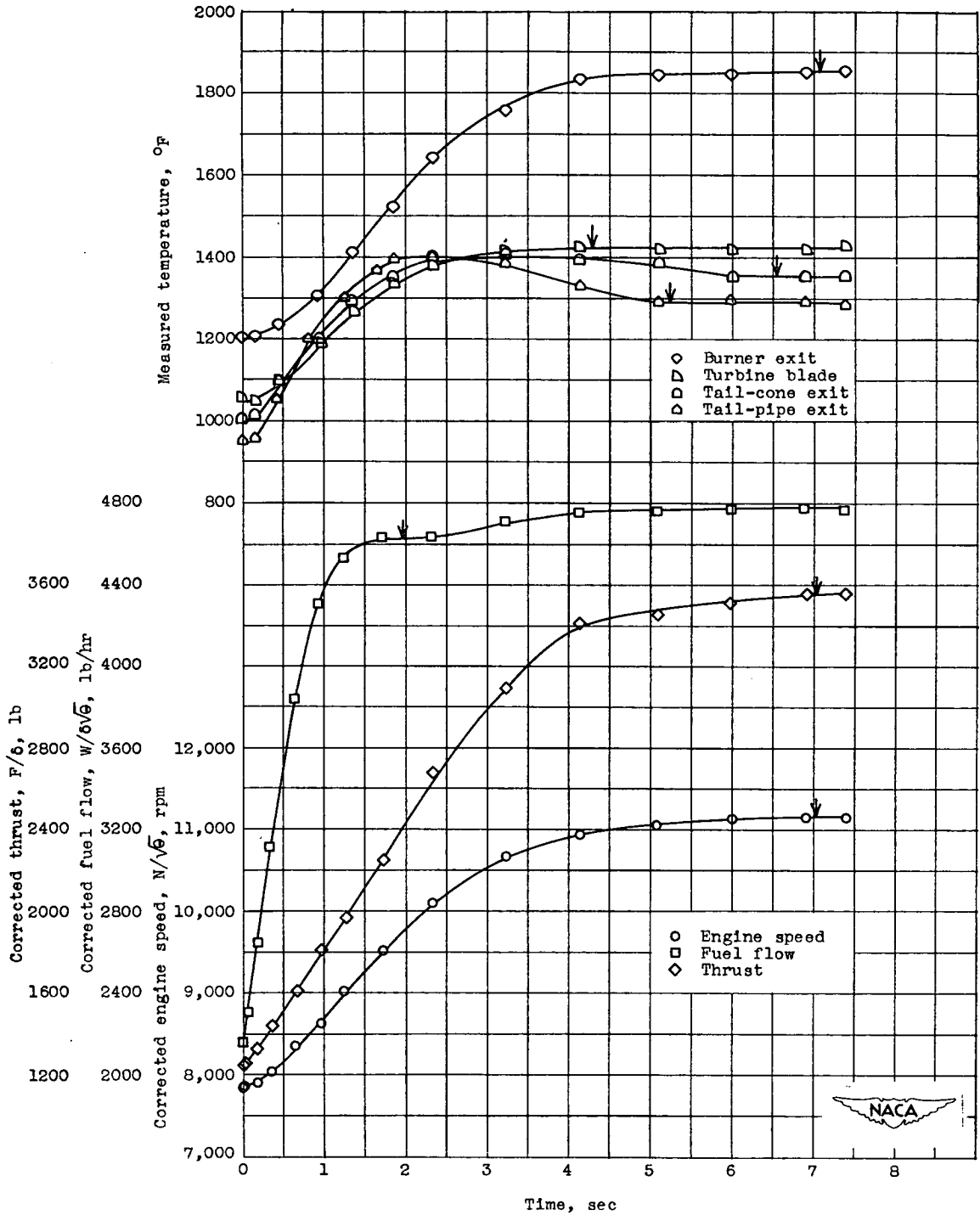
Figure 7. - Continued. Acceleration characteristics with step change in fuel flow corresponding to change in uncorrected engine speed. Arrows indicate time at which equilibrium is reached.





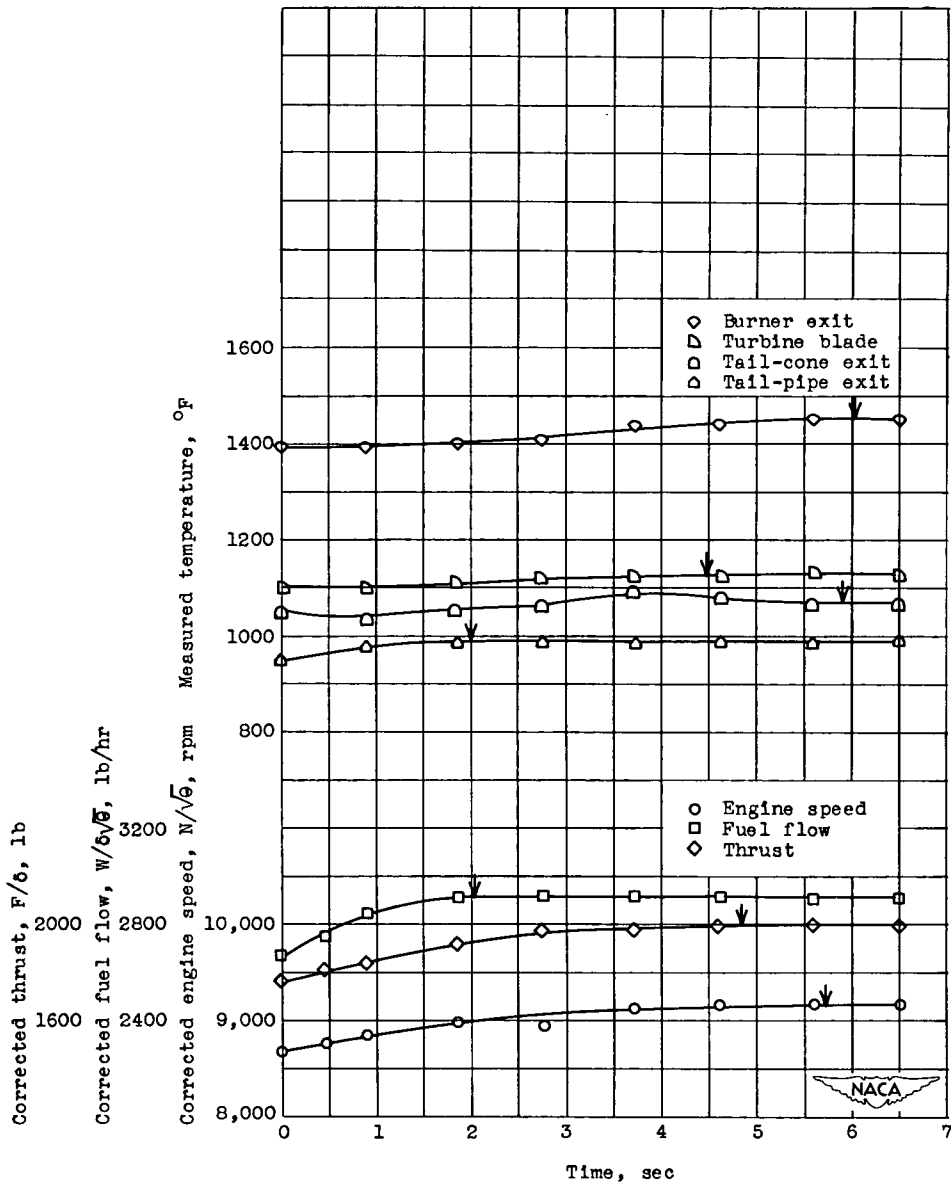
(d) Acceleration, 8,000 to 11,000 rpm;  $\sqrt{\delta}$ , 1.020;  $\delta$ , 0.974.

Figure 7. - Continued. Acceleration characteristics with step change in fuel flow corresponding to change in uncorrected engine speed. Arrows indicate time at which equilibrium is reached.



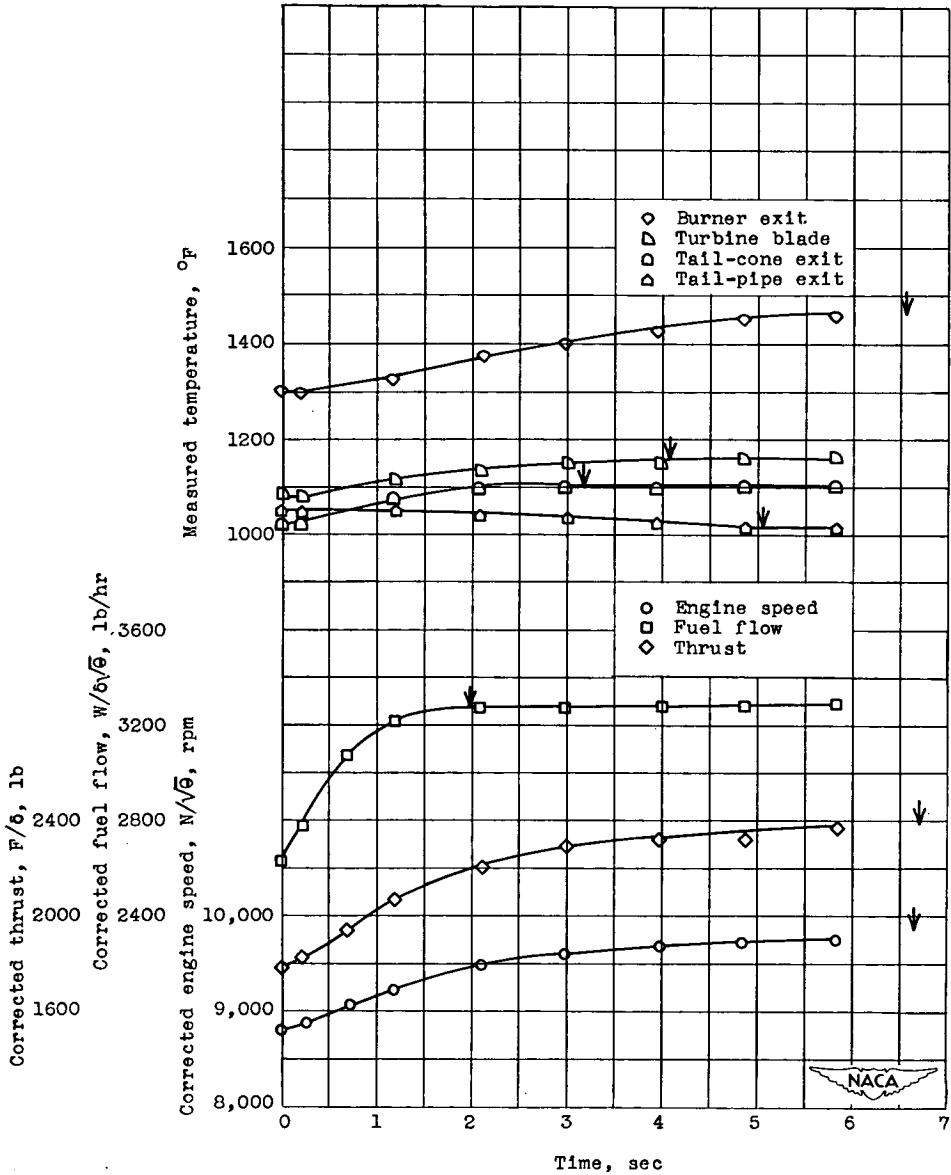
(e) Acceleration, 8,000 to 11,500 rpm;  $\sqrt{\theta}$ , 1.025;  $\delta$ , 0.975.

Figure 7. - Continued. Acceleration characteristics with step change in fuel flow corresponding to change in uncorrected engine speed. Arrows indicate time at which equilibrium is reached.



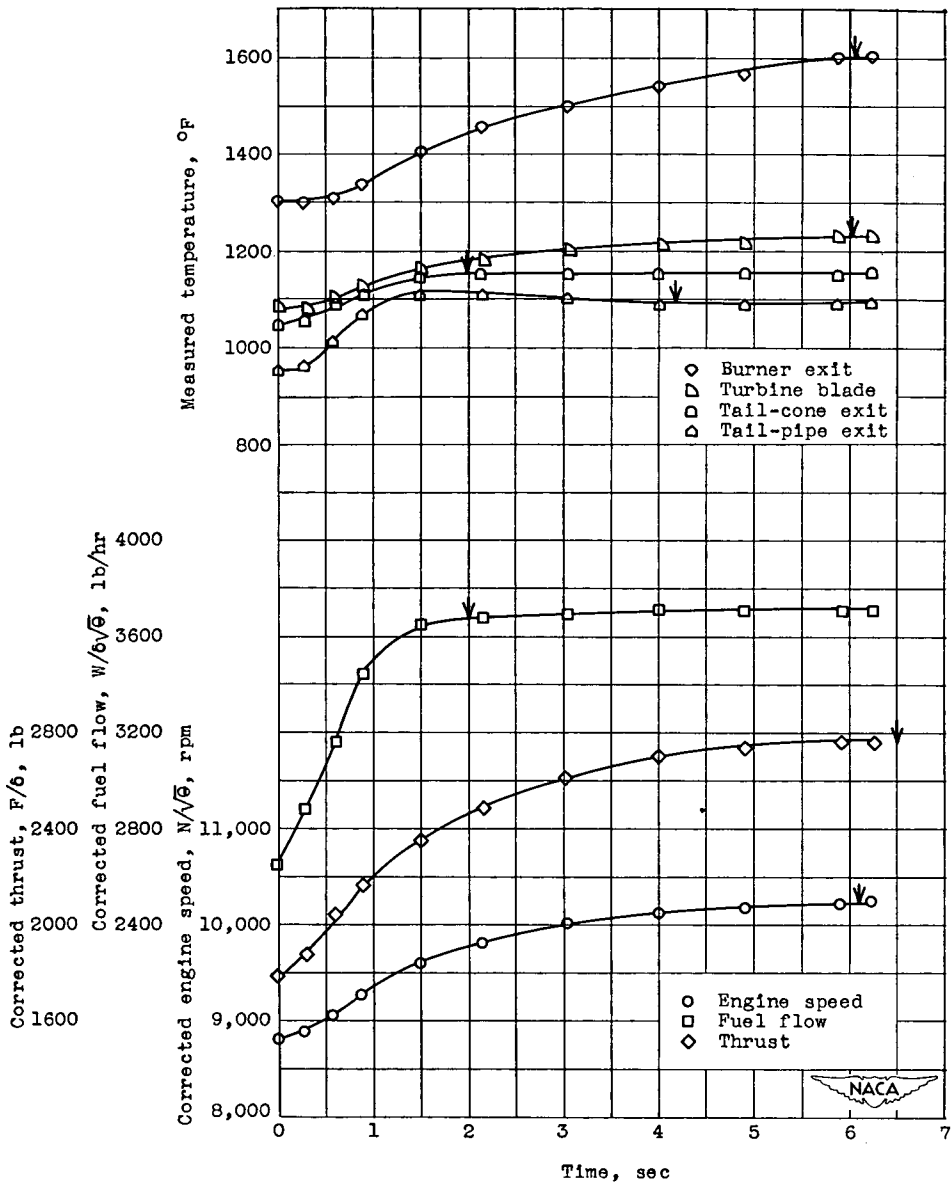
(f) Acceleration, 9000 to 9500 rpm;  $\sqrt{\theta}$ , 1.035;  $\delta$ , 0.976.

Figure 7. - Continued. Acceleration characteristics with step change in fuel flow corresponding to change in uncorrected engine speed. Arrows indicate time at which equilibrium is reached.



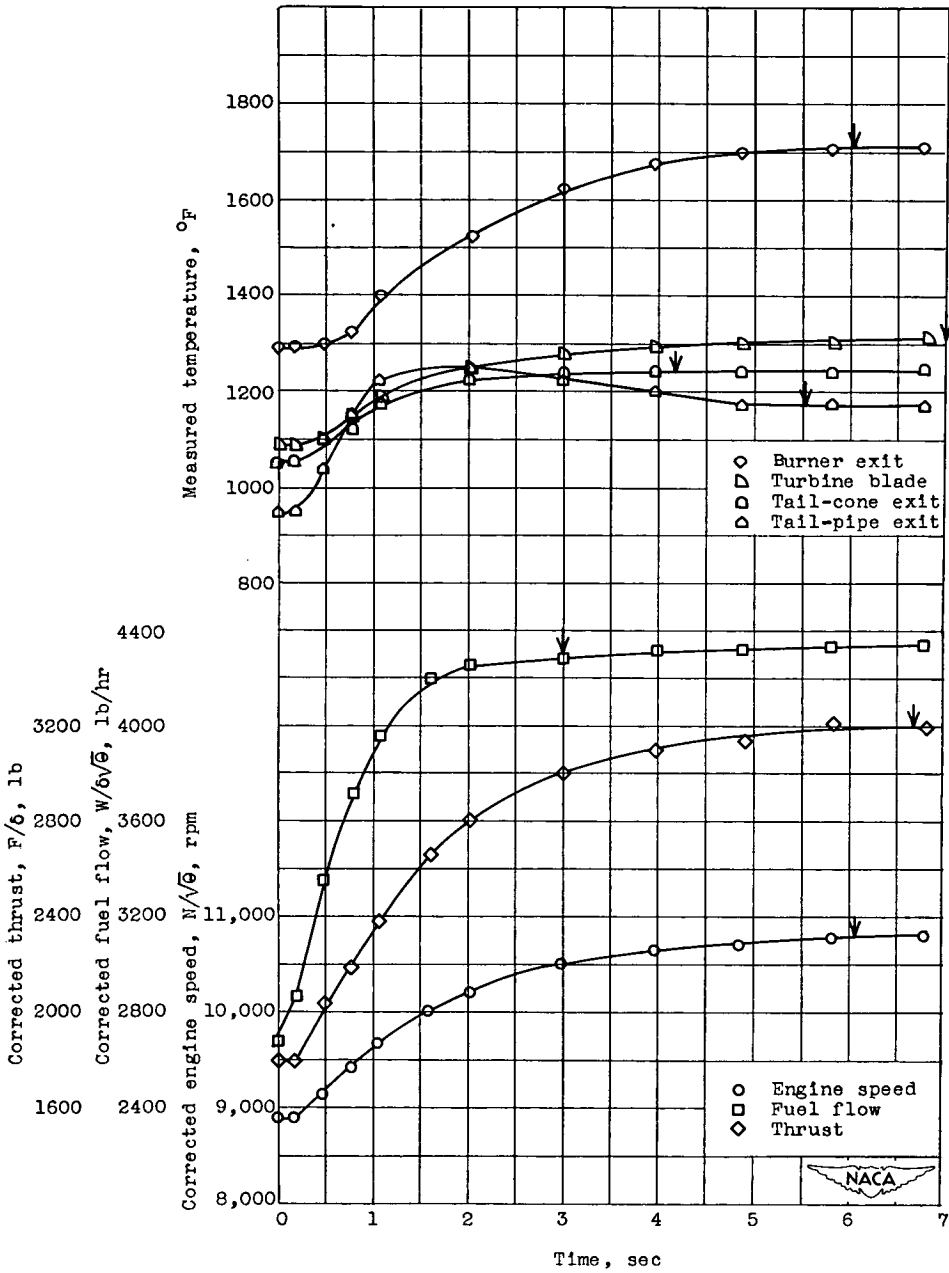
(g) Acceleration, 9,000 to 10,000 rpm;  
 $\sqrt{\theta}$ , 1.025;  $\delta$ , 0.974.

Figure 7. - Continued. Acceleration characteristics with step change in fuel flow corresponding to change in uncorrected engine speed. Arrows indicate time at which equilibrium is reached.



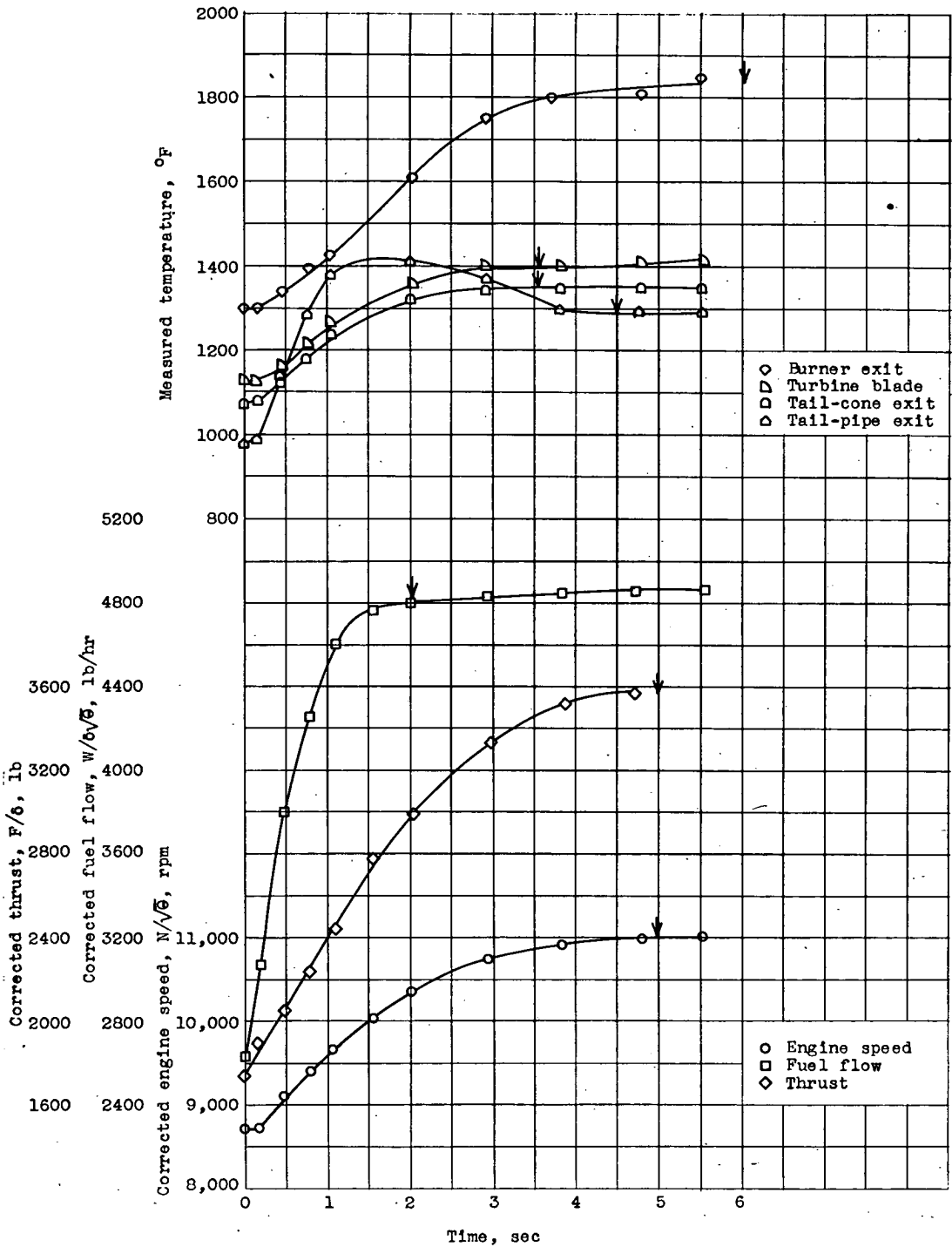
(h) Acceleration, 9,000 to 10,500 rpm;  $\sqrt{\theta}$ , 1.025;  $\delta$ , 0.974.

Figure 7. - Continued. Acceleration characteristics with step change in fuel flow corresponding to change in uncorrected engine speed. Arrows indicate time at which equilibrium is reached.



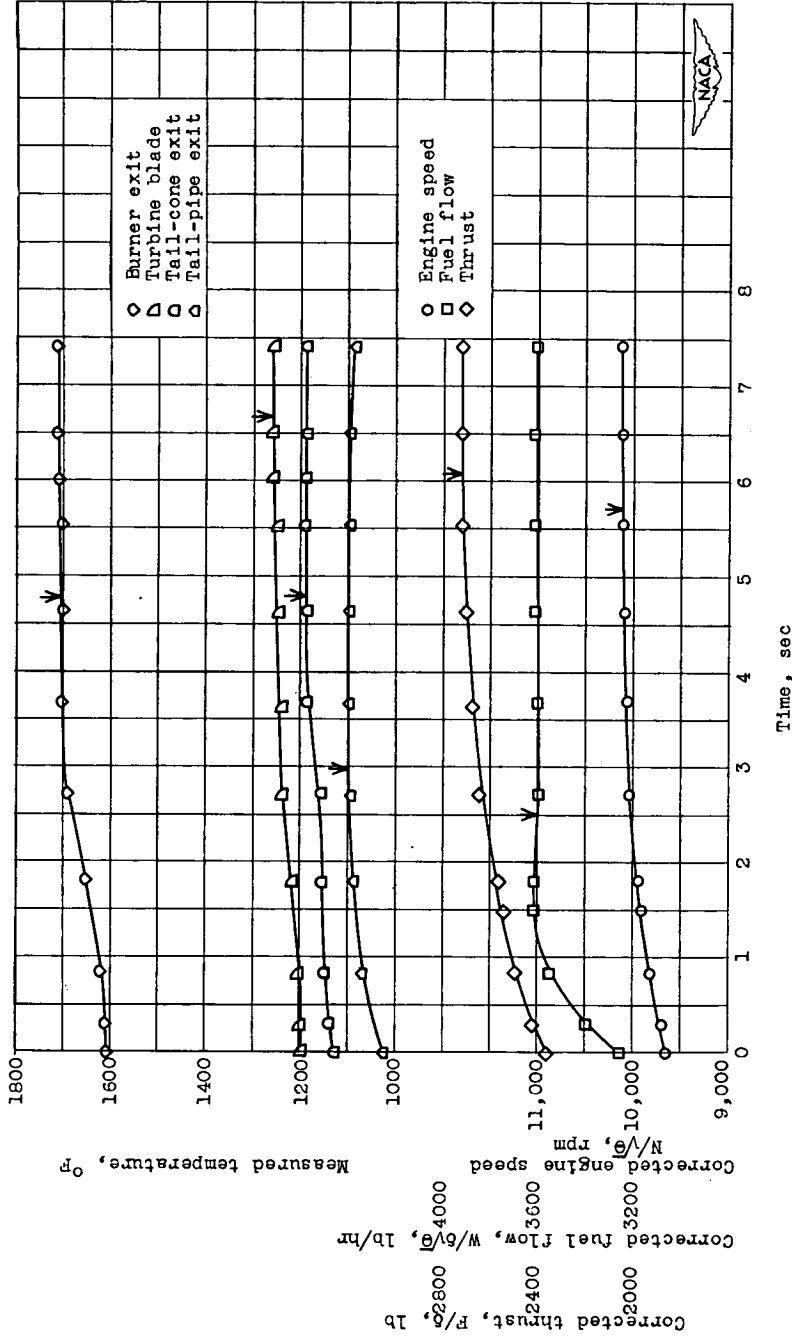
(i) Acceleration, 9,000 to 11,000 rpm;  $\sqrt{\delta}$ , 1.020;  $\delta$ , 0.974.

Figure 7. - Continued. Acceleration characteristics with step change in fuel flow corresponding to change in uncorrected engine speed. Arrows indicate time at which equilibrium is reached.



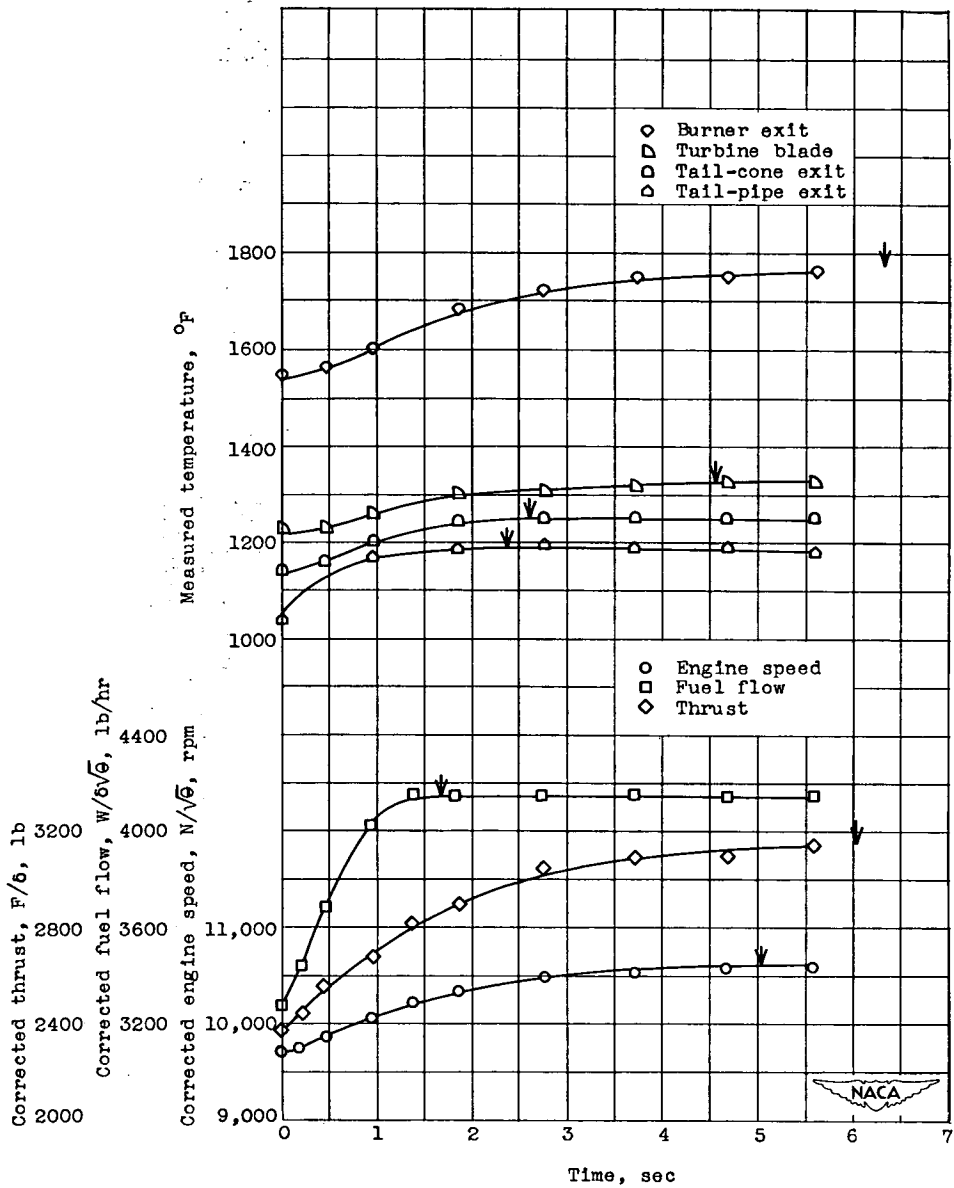
(j) Acceleration, 9,000 to 11,500 rpm;  $\sqrt{\sigma}$ , 1.035;  $\delta$ , 0.970.

Figure 7. - Continued. Acceleration characteristics with step change in fuel flow corresponding to change in uncorrected engine speed. Arrows indicate time at which equilibrium is reached.



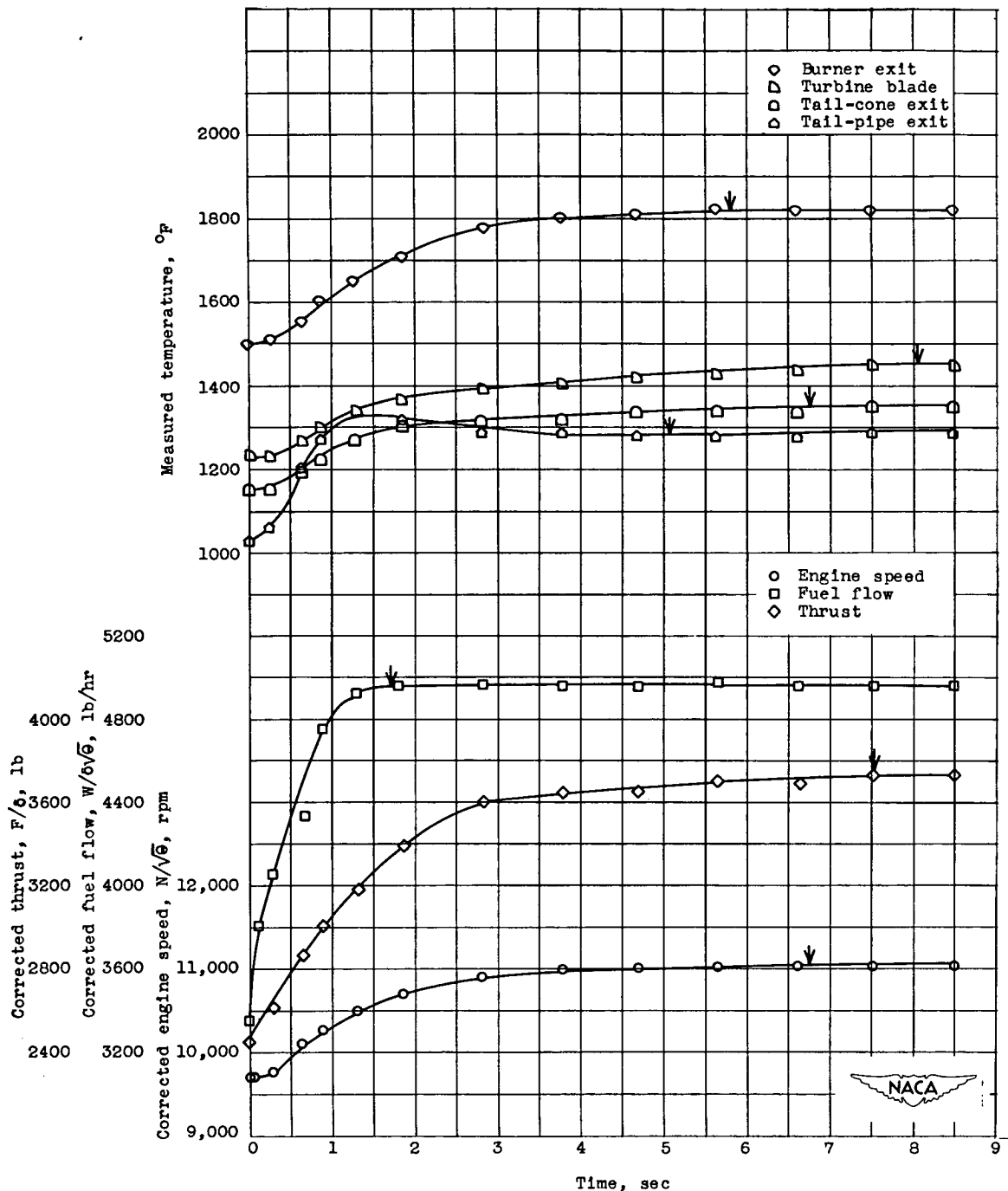
(k) Acceleration, 10,000 to 10,500 rpm;  $\sqrt{6}$ , 1.035;  $\delta$ , 0.976.

Figure 7. - Continued. Acceleration characteristics with step change in fuel flow corresponding to change in uncorrected engine speed. Arrows indicate time at which equilibrium is reached.



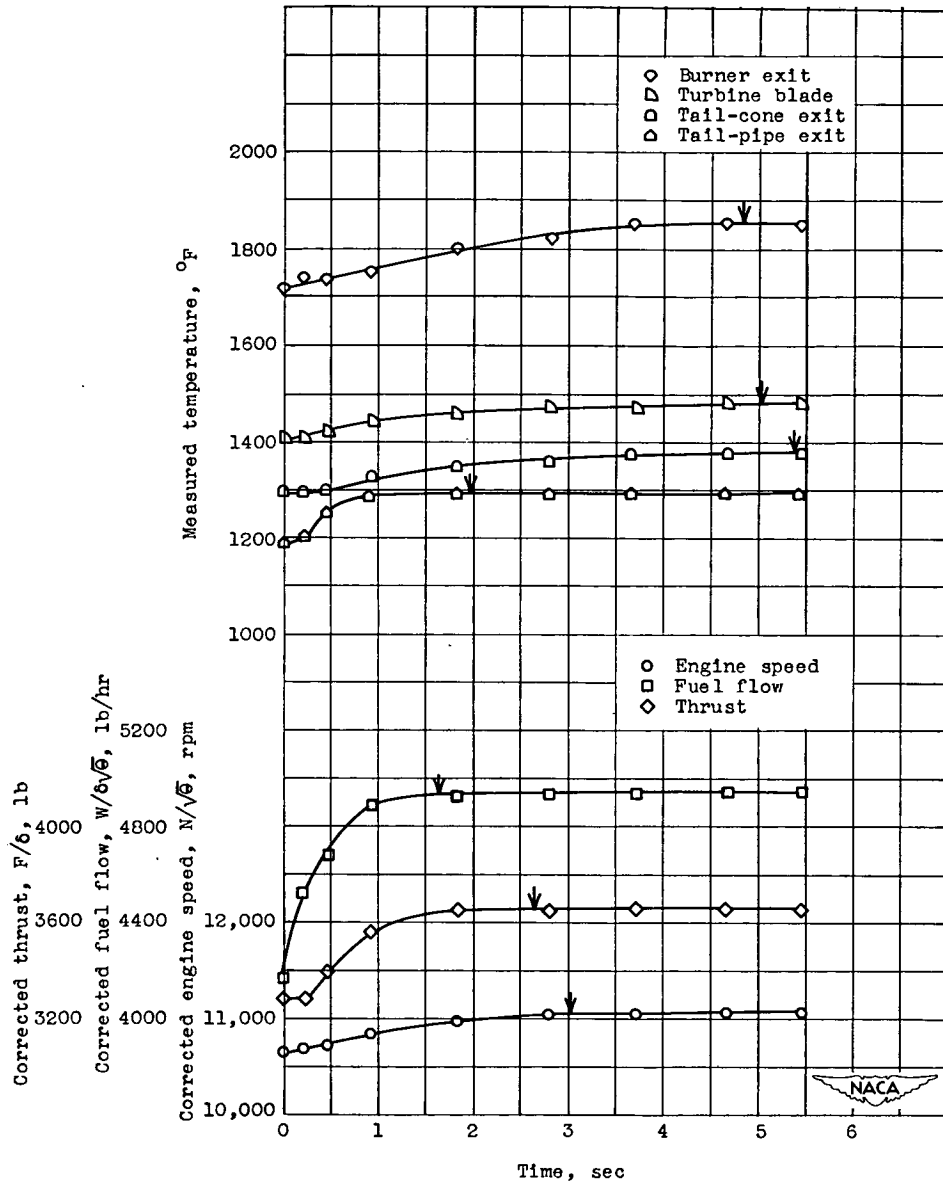
(1) Acceleration, 10,000 to 11,000 rpm;  $\sqrt{\delta}$ , 1.035;  $\delta$ , 0.976.

Figure 7. - Continued. Acceleration characteristics with step change in fuel flow corresponding to change in uncorrected engine speed. Arrows indicate time at which equilibrium is reached.



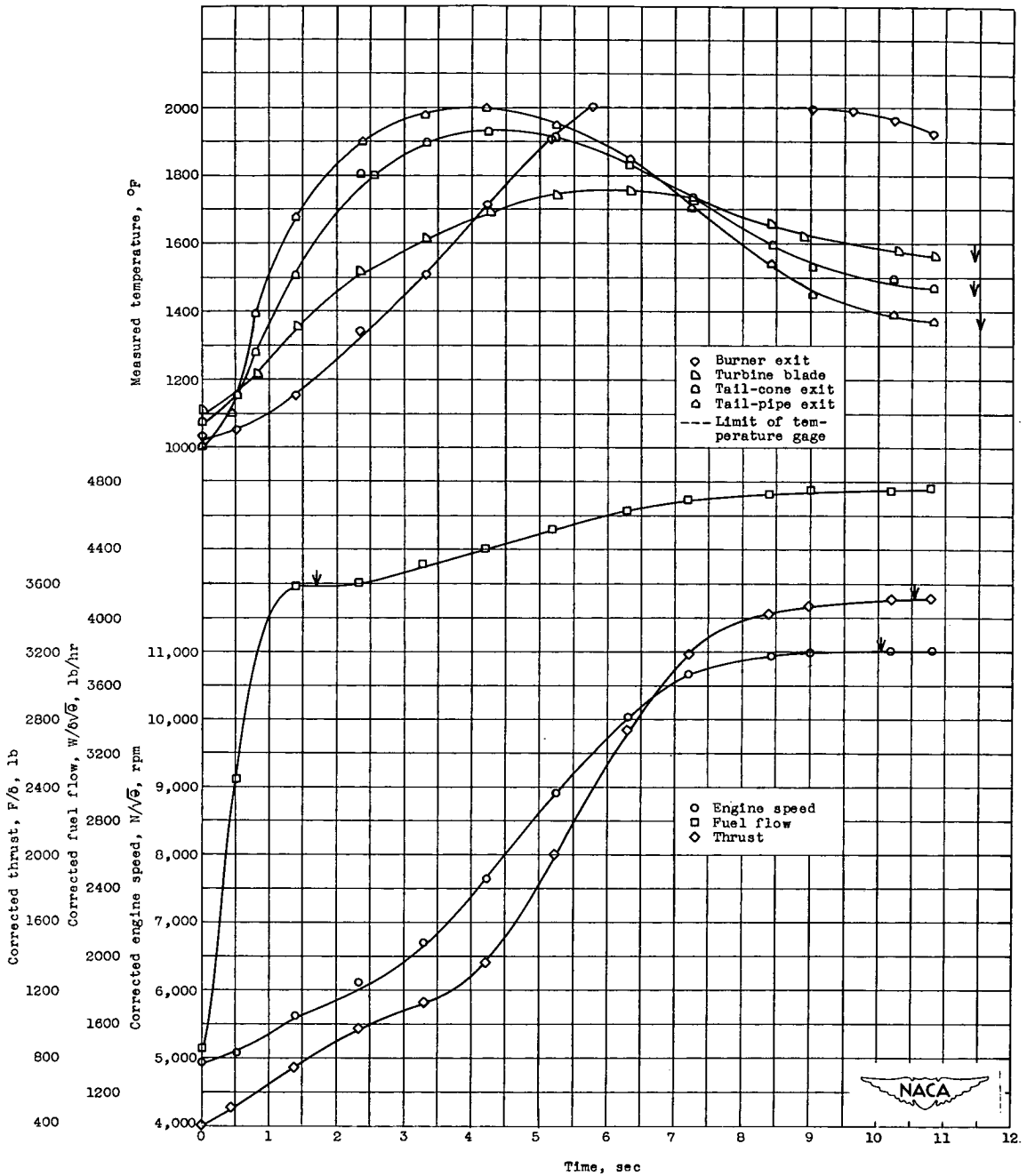
(m) Acceleration, 10,000 to 11,500 rpm;  $\sqrt{\theta}$ , 1.036;  $\delta$ , 0.974.

Figure 7. - Continued. Acceleration characteristics with step change in fuel flow corresponding to change in uncorrected engine speed. Arrows indicate time at which equilibrium is reached.



(n) Acceleration, 11,000 to 11,500 rpm;  
 $\sqrt{\theta}$ , 1.036;  $\delta$ , 0.974.

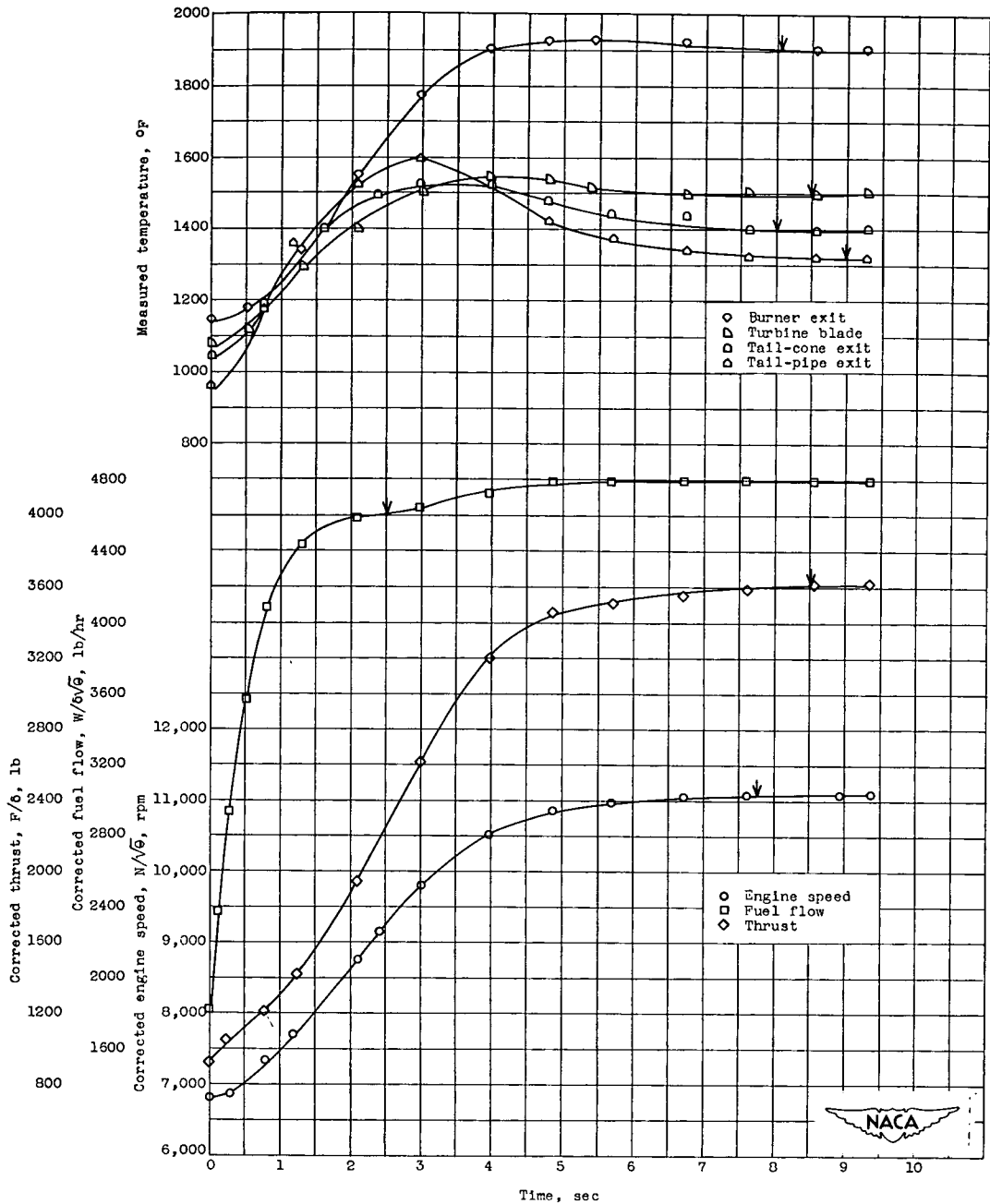
Figure 7. - Continued. Acceleration characteristics with step change in fuel flow corresponding to change in uncorrected engine speed. Arrows indicate time at which equilibrium is reached.



(c) Acceleration, 5,000 to 11,500 rpm;  $\sqrt{\theta}$ , 1.031;  $\delta$ , 0.9851.

Figure 7. - Continued. Acceleration characteristics with step change in fuel flow corresponding to change in uncorrected engine speed. Arrows indicate time at which equilibrium is reached.

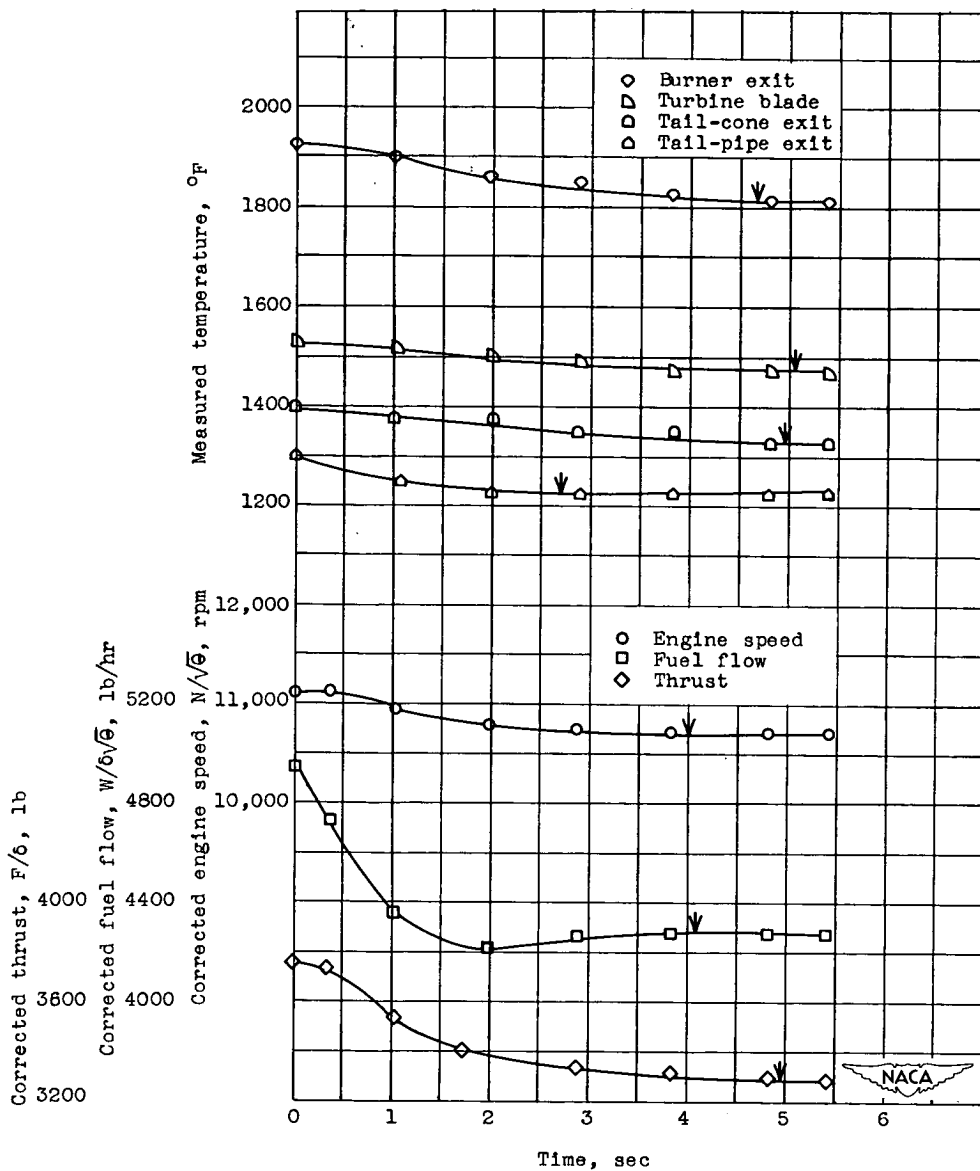




(p) Acceleration, 7,000 to 11,500 rpm;  $\sqrt{g}$ , 1.031;  $\delta$ , 0.9715.

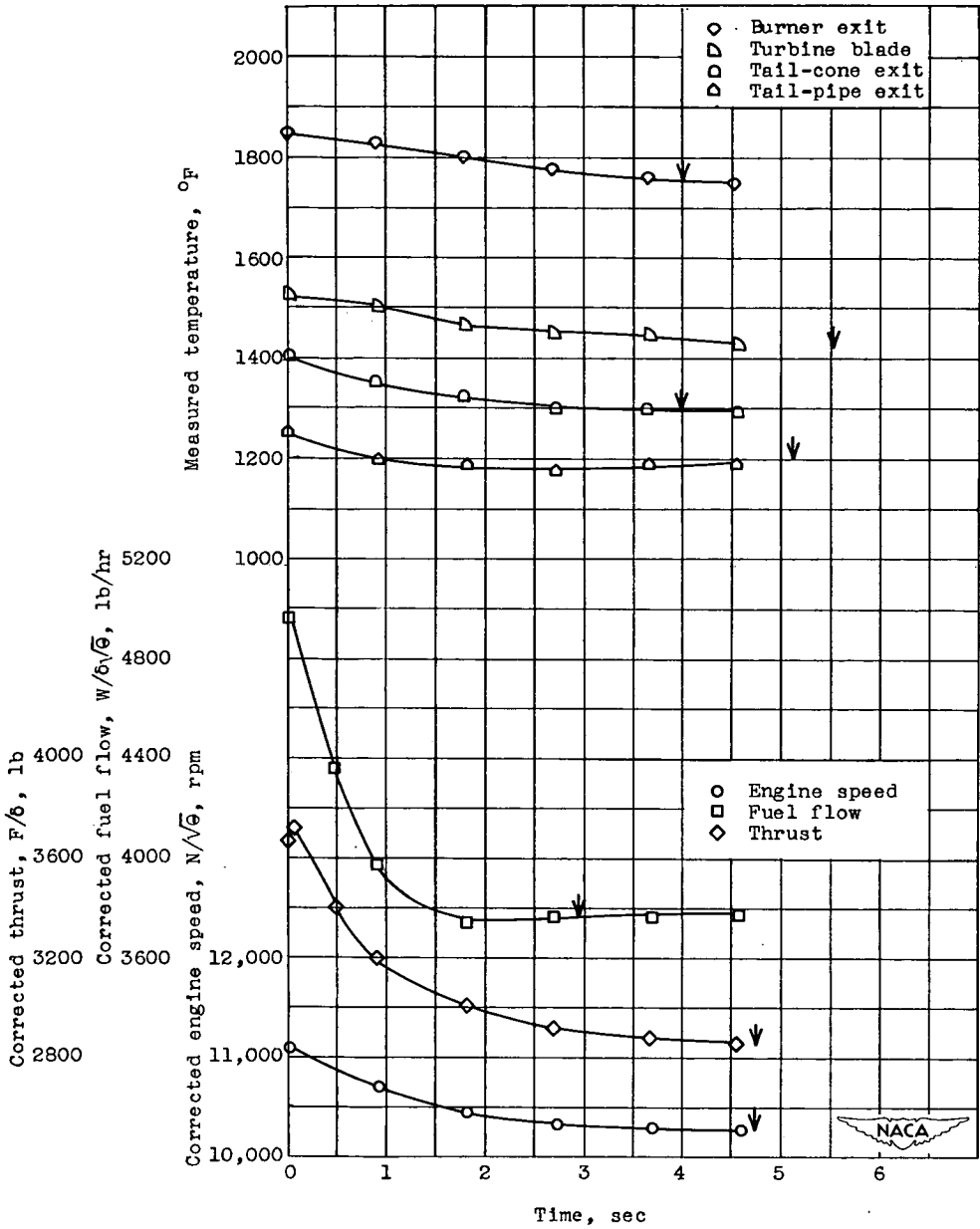
Figure 7. - Concluded. Acceleration characteristics with step change in fuel flow corresponding to change in uncorrected engine speed. Arrows indicate time at which equilibrium is reached.





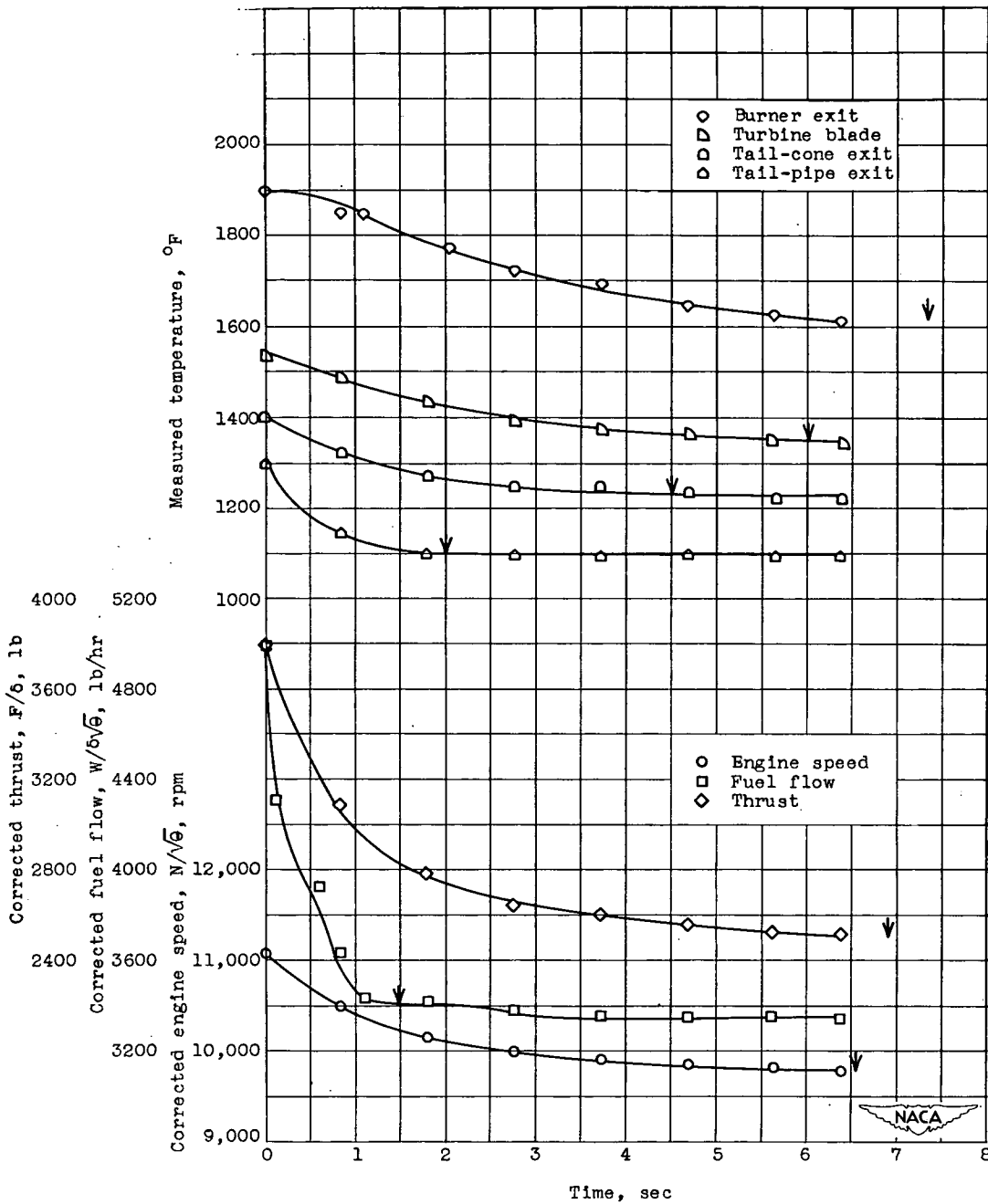
(a) Deceleration, 11,500 to 11,000 rpm,  
 $\sqrt{\theta}$ , 1.036;  $\delta$ , 0.9739.

Figure 8. - Deceleration characteristics with step change in fuel flow corresponding to change in uncorrected engine speed. Arrows indicate time at which equilibrium is reached.



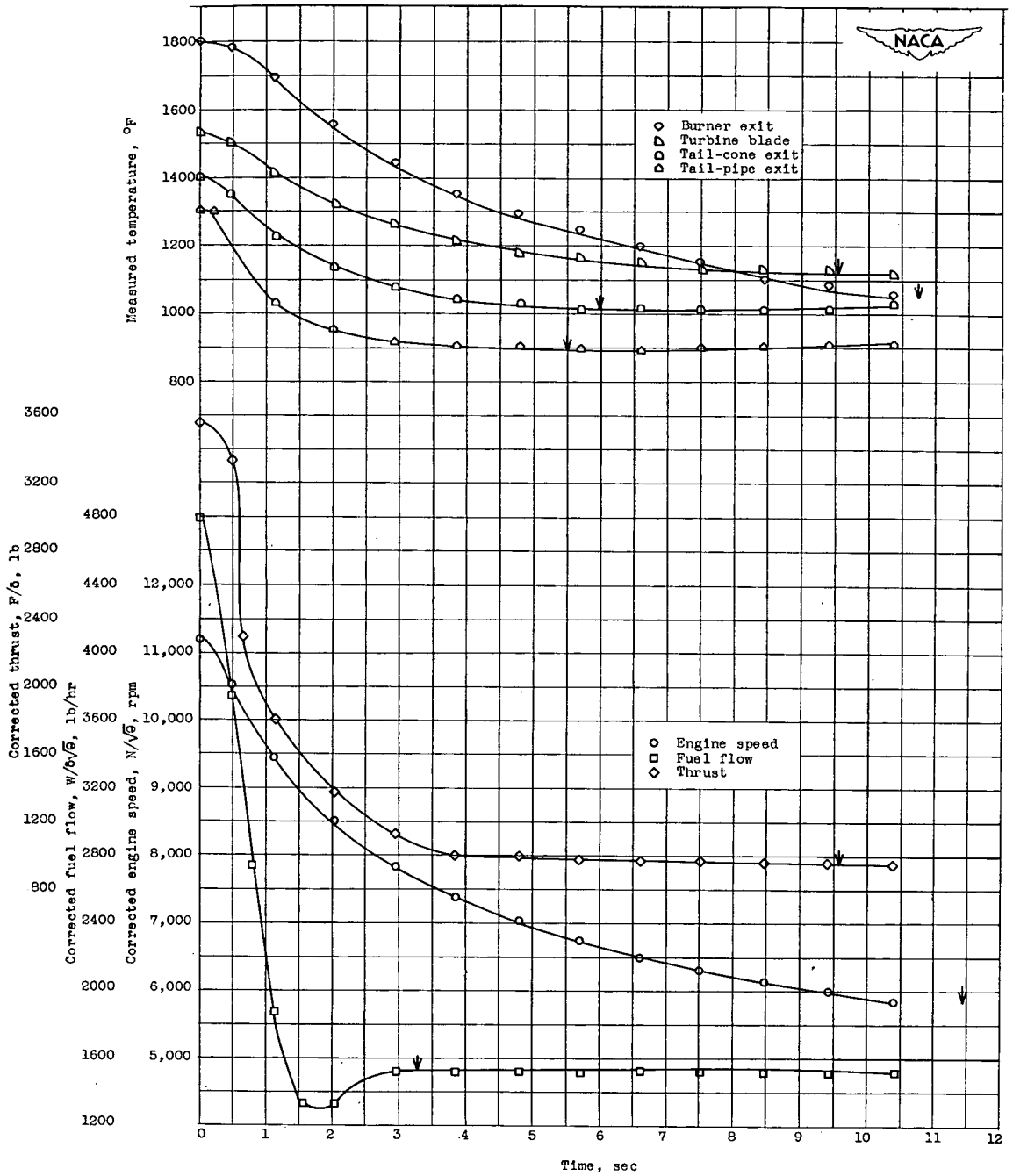
(b) Deceleration, 11,500 to 10,500 rpm;  
 $\sqrt{\delta}$ , 1.035;  $\delta$ , 0.9699.

Figure 8. - Continued. Deceleration characteristics with step change in fuel flow corresponding to change in uncorrected engine speed. Arrows indicate time at which equilibrium is reached.



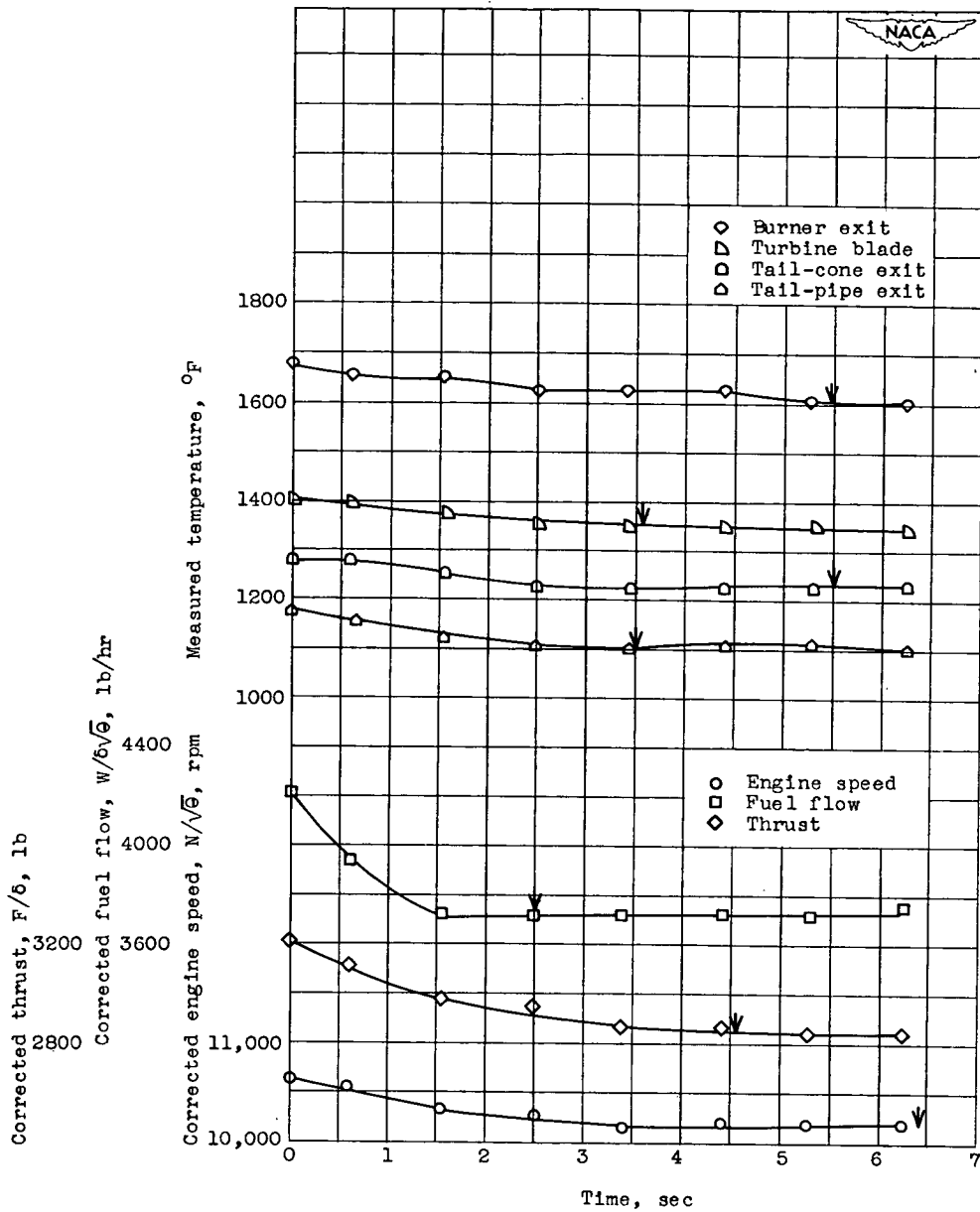
(c) Deceleration, 11,500 to 10,000 rpm;  $\sqrt{\theta}$ , 1.036;  $\delta$ , 0.9739.

Figure 8. - Continued. Deceleration characteristics with step change in fuel flow corresponding to change in uncorrected engine speed. Arrows indicate time at which equilibrium is reached.



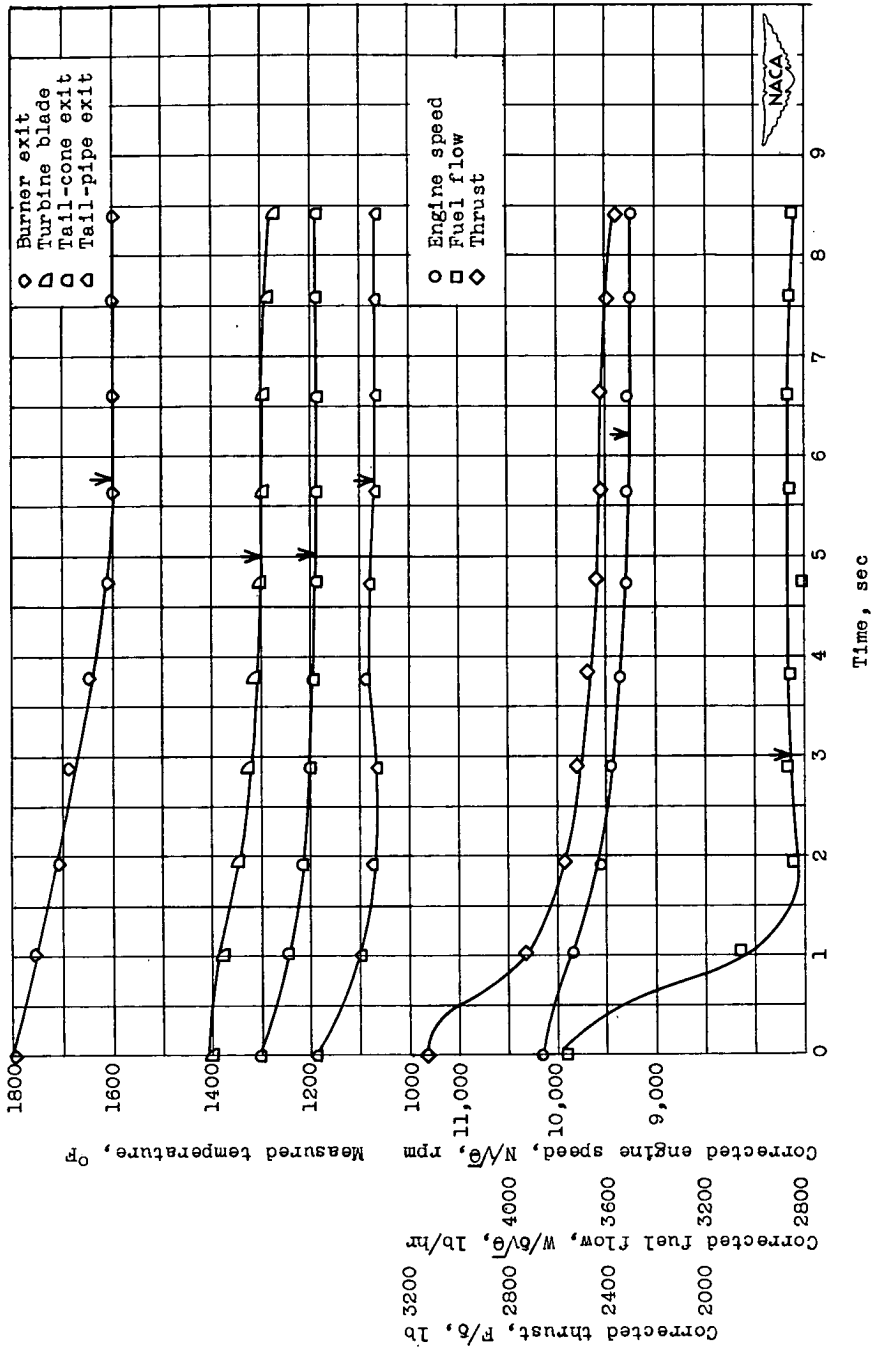
(d) Deceleration, 11,500 to 5,000 rpm;  $\sqrt{\theta}$ , 1.028;  $\delta$ , 0.9853.

Figure 8. - Continued. Deceleration characteristics with step change in fuel flow corresponding to change in uncorrected engine speed. Arrows indicate time at which equilibrium is reached.



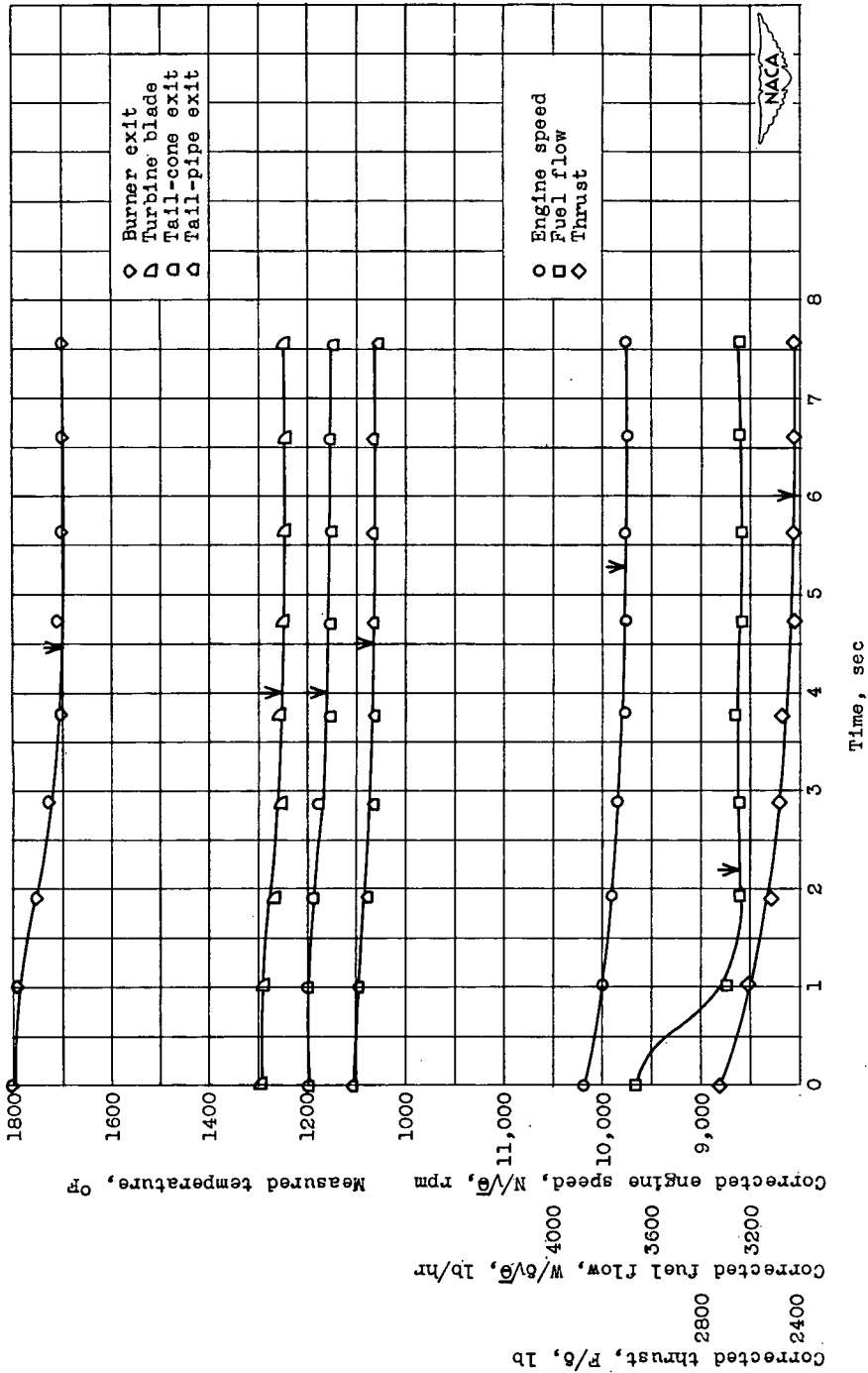
(e) Deceleration, 11,000 to 10,500 rpm;  $\sqrt{\theta}$ , 1.036;  $\delta$ , 0.9739.

Figure 8. - Continued. Deceleration characteristics with step change in fuel flow corresponding to change in uncorrected engine speed. Arrows indicate time at which equilibrium is reached.



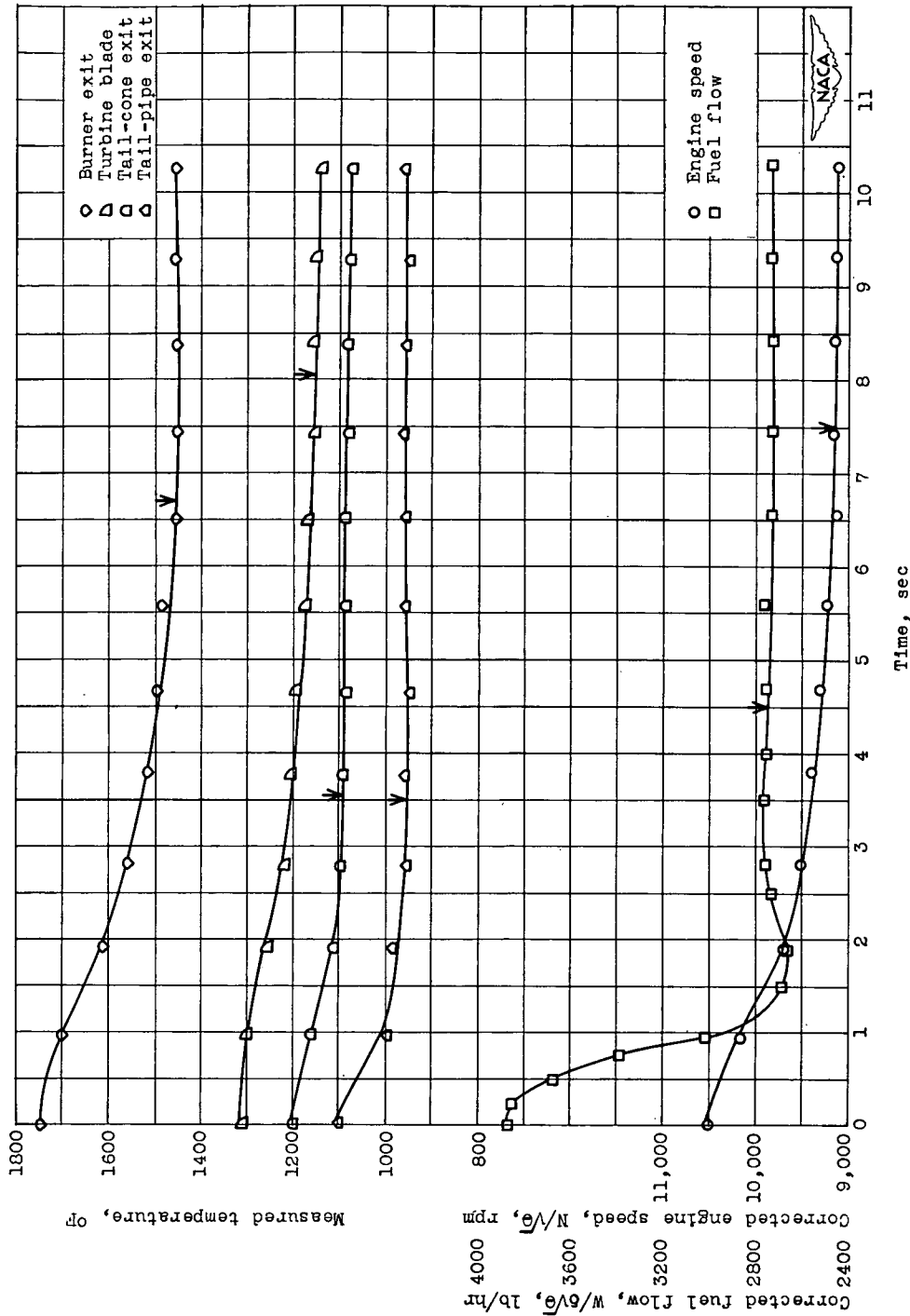
(f) Deceleration, 11,000 to 10,000 rpm;  $\sqrt{\theta}$ , 1.035;  $\delta$ , 0.9759.

Figure 8. - Continued. Deceleration characteristics with step change in fuel flow corresponding to change in uncorrected engine speed. Arrows indicate time at which equilibrium is reached.



(g) Deceleration, 10,500 to 10,000 rpm;  $\sqrt{\theta}$ , 1.035;  $\theta$ , 0.9759.

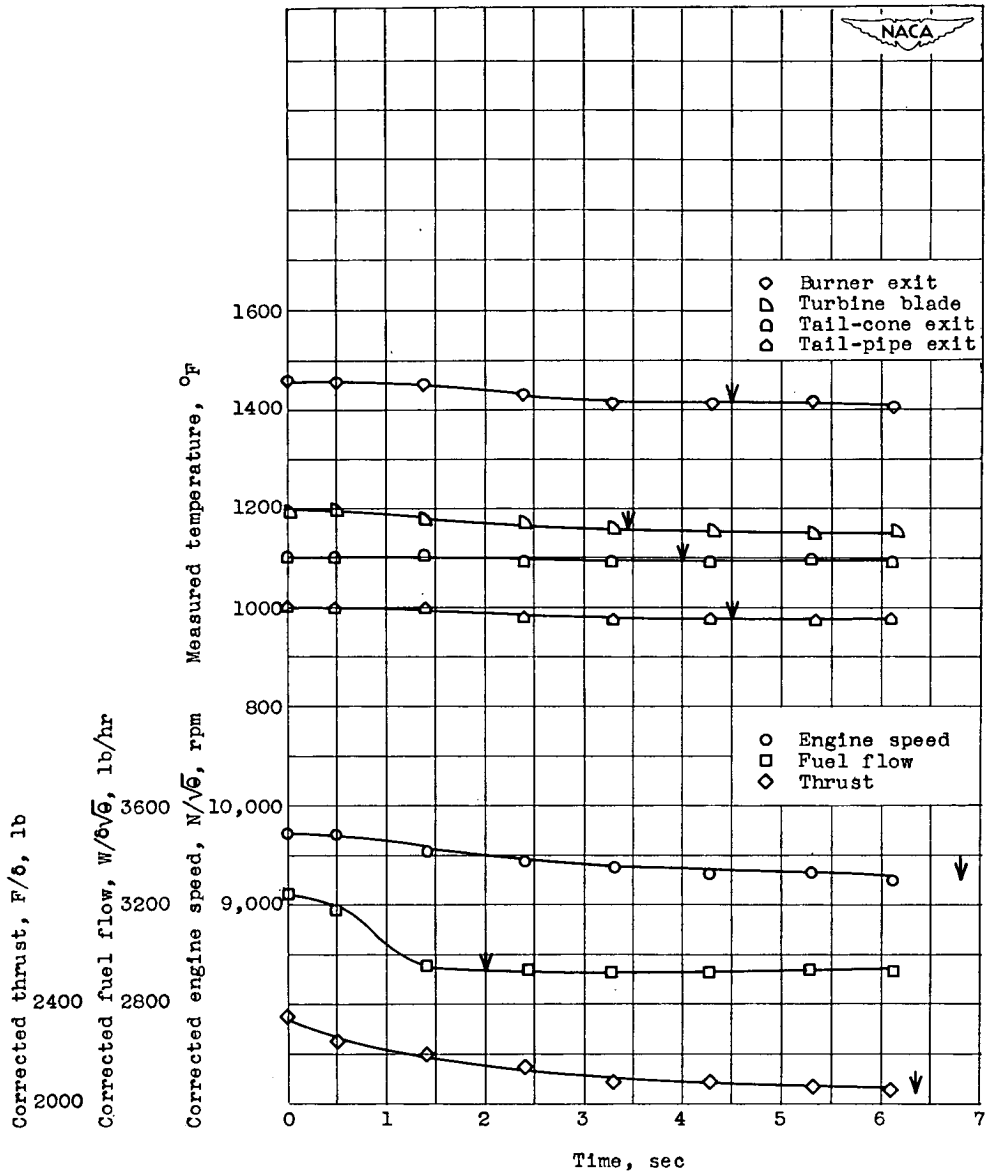
Figure 8. - Continued. Deceleration characteristics with step change in fuel flow corresponding to change in uncorrected engine speed. Arrows indicate time at which equilibrium is reached.



(h) Deceleration, 10,500 to 9,000 rpm;  $\sqrt{\theta}$ , 0.9990;  $\delta$ , 0.9759.

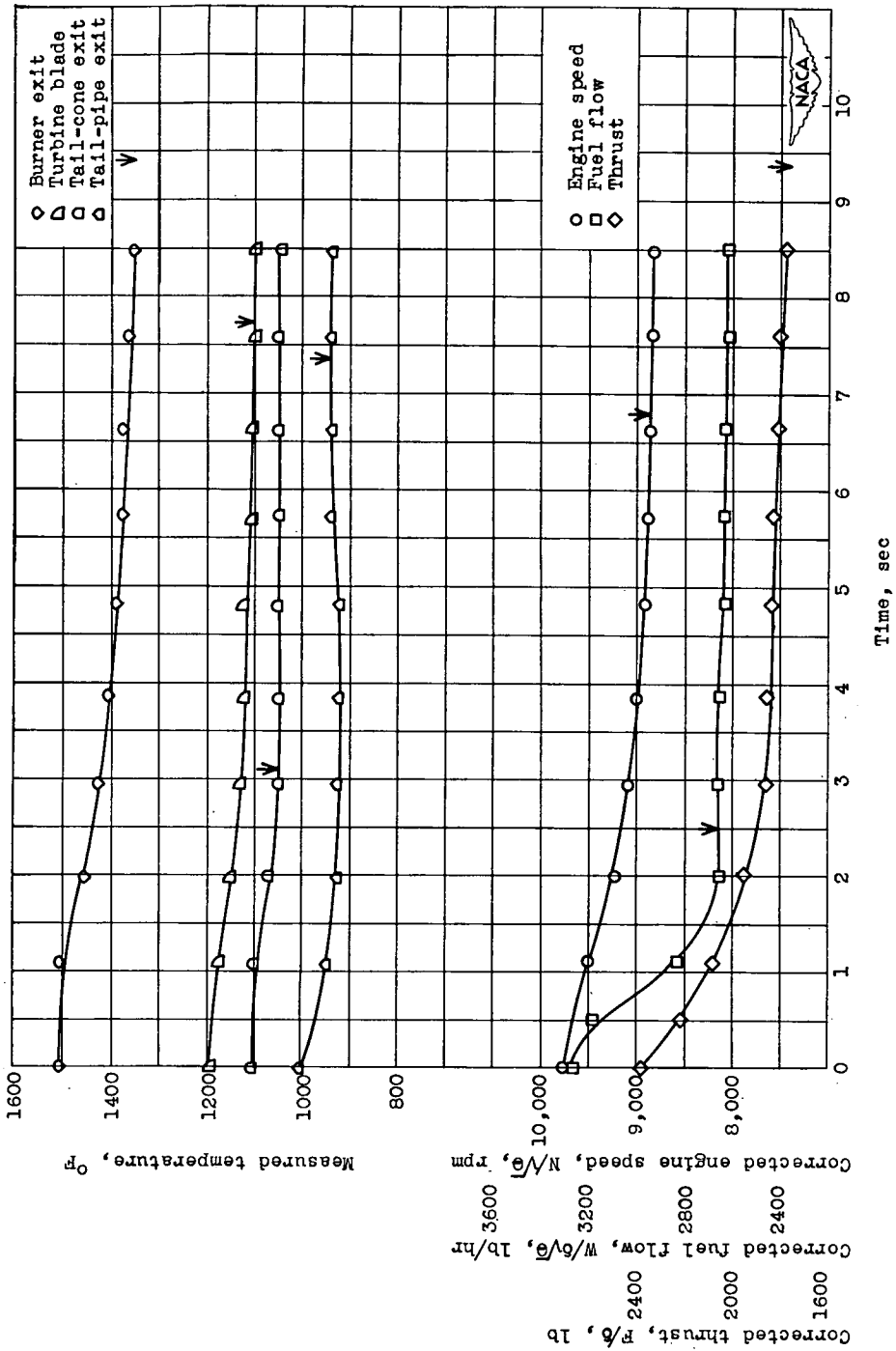
Figure 8. - Continued. Deceleration characteristics with step change in fuel flow corresponding to change in uncorrected engine speed. Arrows indicate time at which equilibrium is reached.





(1) Deceleration, 10,000 to 9,500 rpm;  
 $\sqrt{\theta}$ , 1.030;  $\delta$ , 0.9743.

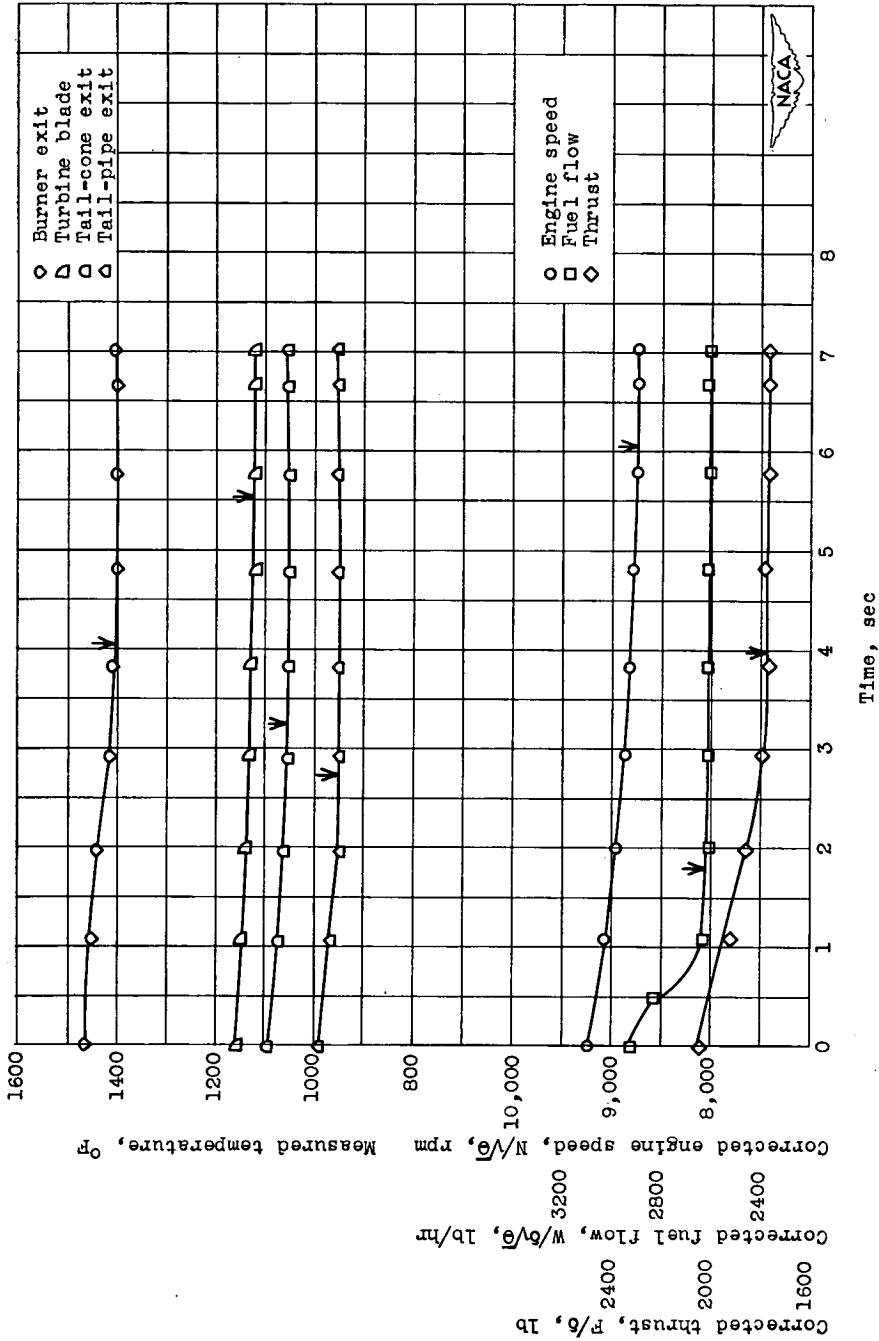
Figure 8. - Continued. Deceleration characteristics with step change in fuel flow corresponding to change in uncorrected engine speed. Arrows indicate time at which equilibrium is reached.



(j) Deceleration, 10,000 to 9,000 rpm;  $\sqrt{6}$ , 1.030;  $\delta$ , 0.9743.

Figure 8. - Continued. Deceleration characteristics with step change in fuel flow corresponding to change in uncorrected engine speed. Arrows indicate time at which equilibrium is reached.

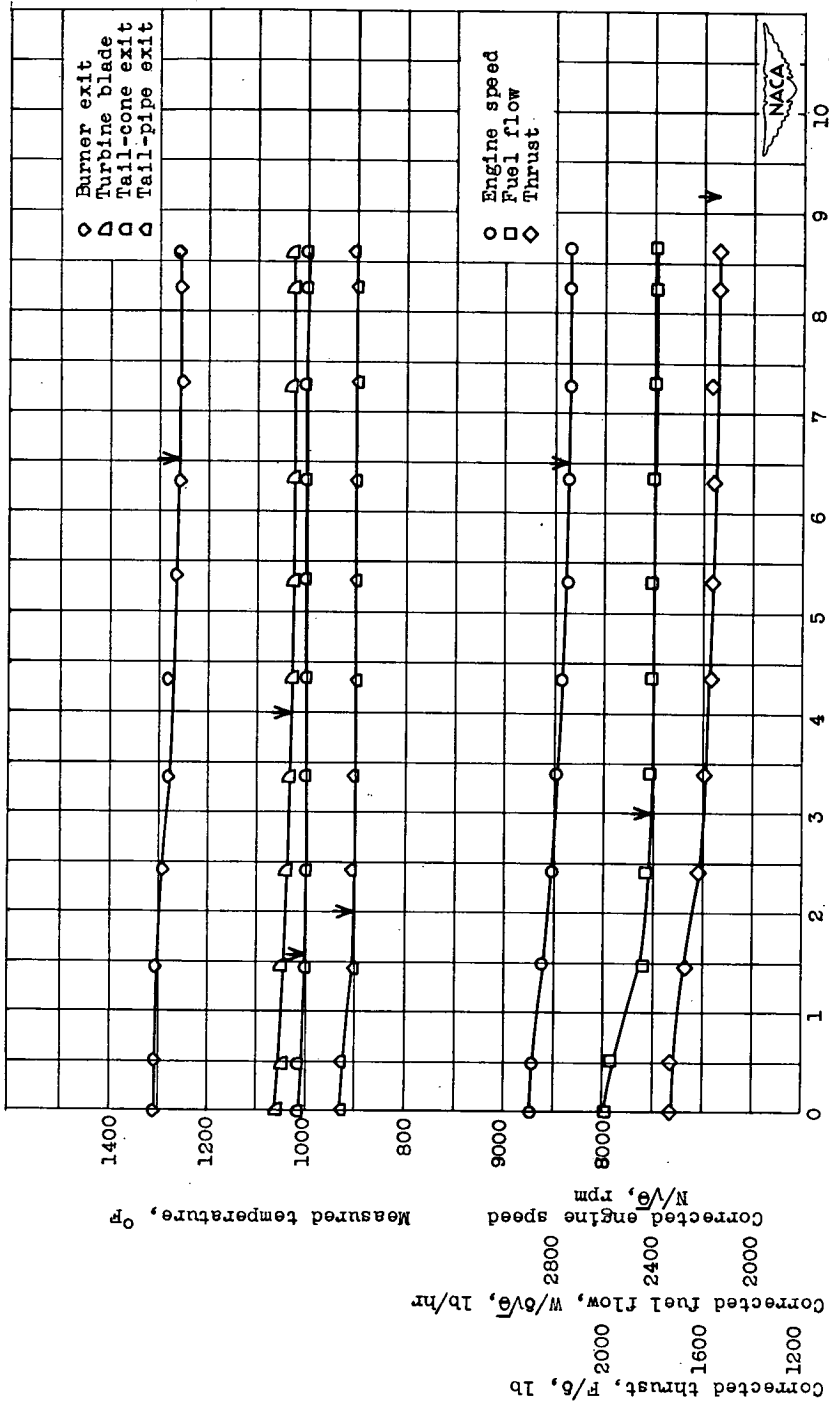




(k) Deceleration, 9500 to 9000 rpm;  $\sqrt{\theta}$ , 1.035;  $\delta$ , 0.9759.

Figure 8. - Continued. Deceleration characteristics with step changes in fuel flow corresponding to change in uncorrected engine speed. Arrows indicate time at which equilibrium is reached.

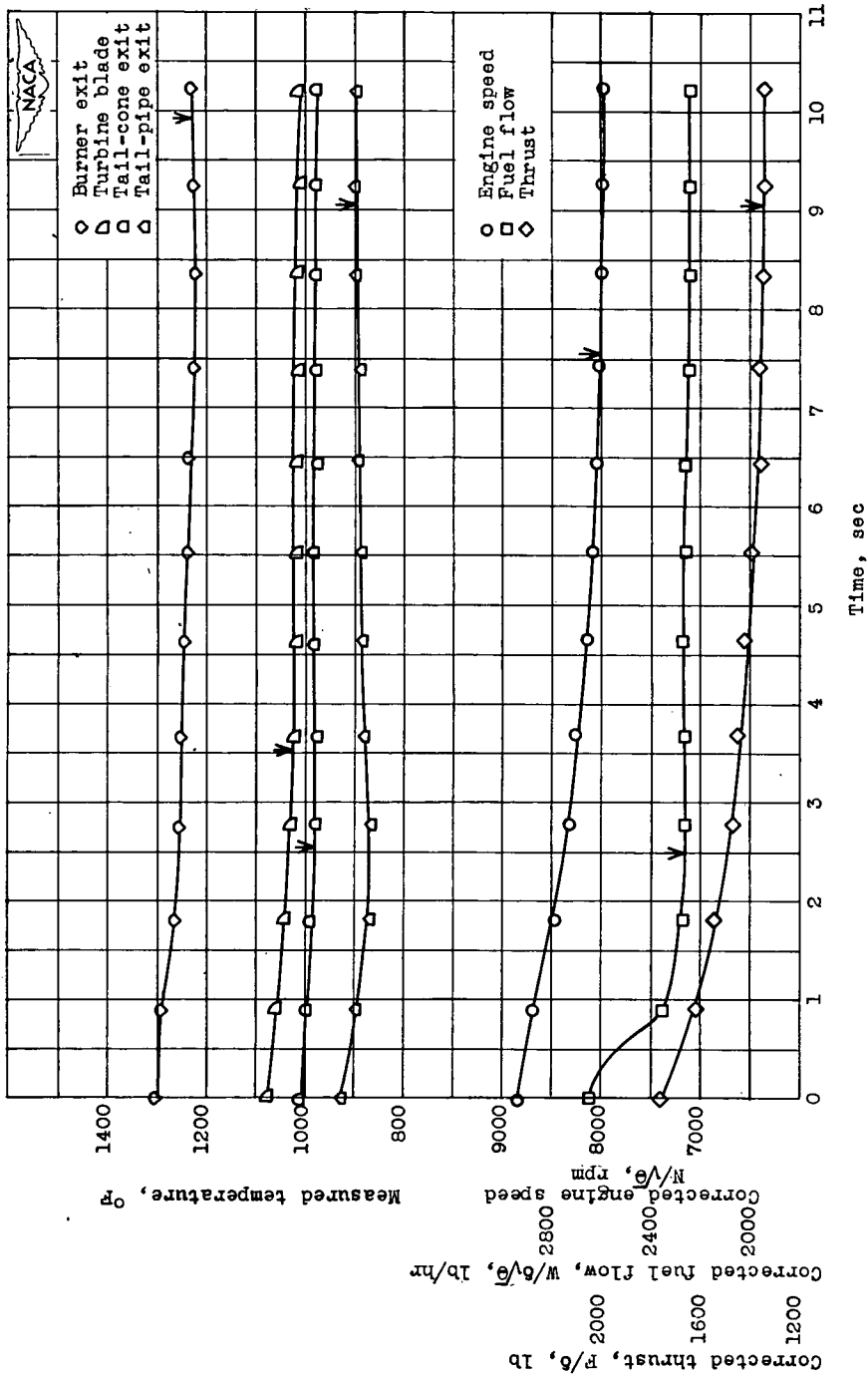




(1) Deceleration, 9000 to 8500 rpm;  $\sqrt{6}$ , 1.030;  $\delta$ , 0.9743.

Figure 8. - Continued. Deceleration characteristics with step change in fuel flow corresponding to change in uncorrected engine speed. Arrows indicate time at which equilibrium is reached.





(m) Deceleration, 9000 to 8000 rpm;  $\sqrt{6}$ , 1.020;  $\delta$ , 0.9743.

Figure 8. - Concluded. Deceleration characteristics with step change in fuel flow corresponding to change in uncorrected engine speed. Arrows indicate time at which equilibrium is reached.